Contemporary Mathematics
https://ojs.wiserpub.com/index.php/CM/

Research Article

Dynamics of Predator-Prey Models with Negative Direct Effects of Climate Change

Jawdat Alebraheem

Department of Mathematics, College of Sciences, Majmaah University, Al-Majmaah, 11952, Saudi Arabia
E-mail: j.alebraheem@mu.edu.sa

Received: 27 February 2025; **Revised:** 8 April 2025; **Accepted:** 23 April 2025

Abstract: The impact of climate change has become a very important topic and can have a direct impact on predator-prey interactions. Therefore, in this paper, we introduce a novel competitive predator-prey model under the negative effects of climate change. Based on their different properties, Holling type I and II functional responses are considered to be two different models for studying dynamic behaviors. Two approaches to the negative impacts of climate change are assumed: static and periodic changes. Firstly, models with negative climate change are taken as static changes. The existence, positivity, and boundedness of solutions are established. Local and global stability conditions are obtained for all feasible equilibrium points. The Hopf bifurcation is investigated, by taking climate change constants, as bifurcation parameters, which shows that the model with Holling type I is globally stable whenever there exists an internal equilibrium point. However, the model with Holling type II contains two dynamics: stable and limit cycle dynamics. Uniform persistence is proved, and various extinction scenarios have been analytically yielded. In addition, numerical simulations are used to demonstrate and verify our theoretical findings. Negative climate impacts have a significant impact on system stability as well as on the coexistence and extinction of species. Secondly, models with negative climate change are considered periodic changes taking seasonality into account, which is considered tangible evidence of climate change. The dynamics of these effects are investigated numerically. Due to the existence of seasonality, the dynamics become more complex and different, as there are multiple cycles and chaos, which makes the systems more realistic for describing some environments due to the presence of some environmental impacts. The findings of this study show many undesirable scenarios for predator-prey interactions due to negative climate change. In light of these findings, many phenomena and changes due to negative climate change in ecosystems can be explained and predicted from an ecological point of view.

***Keywords*:** climate change, dynamics, holling types, prey predator models, persistence, extinction, chaos

MSC: 65L05, 34K06, 34K28

1. Introduction

Population models are one of the most important topics in applied mathematics, mathematical biology, and mathematical ecology. They have received considerable attention from researchers because of their importance. One of the most important population models is the predator-prey model. The Lotka [1] and Volterra [2] model is considered the basis for these models. Since then, many researchers have proposed and developed different models to describe and

DOI: https://doi.org/10.37256/cm.6320256644

track the dynamics of different predator-prey interactions in different environments; for instance [3–11]. The problems in this field may seem at first glance simple to follow and describe mathematically, but there are many challenges and difficulties that constitute an open field for many ideas and problems. Mathematical modeling plays a pivotal role in understanding and predicting many environmental phenomena and thus has an important role in various contexts such as controlling disease outbreaks, saving endangered species, etc.

Climate change and its effects are some of the most widely discussed topics these days because of their importance. An important effect of climate change is the presence of many extreme climate events that will have a significant impact on species dynamics in predator-prey systems. The impact of climate change on predator-prey interactions can include adaptation, decrease, or extinction of populations that have not responded adequately to such changes [12–15]. Some ecological studies have shown that climate change has a significant impact on the behavior of prey and predators, which can lead to changes in encounter rates [16], and predation rates [17], and contribute to prey refuges [18]. Global warming caused by human activities is the main cause of climate change, which has negative effects on living organisms and the environment on Earth [19]. In the last century, the Earth's temperature has increased by 0.6 degrees Celsius, but the danger lies if the temperature rises, which may lead to environmental disasters and extreme events [20]. Some ecological studies have addressed the environmental impact of climate change on species. Climate change also reduces the biodiversity of predator-prey interactions as well as the rate of encounters, which can lead to destabilization and extinction [15, 17, 18, 21].

In the environment, seasonality refers to periodic changes in any parameters of any ecosystem over time. Seasonality expresses seasonal fluctuations and changes in ecosystems. Therefore, understanding the relationship between the magnitude of fluctuations in ecosystems and the complexity of the system is an important issue. Seasonality has been examined in many studies on predator-prey systems, which showed important results in the diversity of dynamic behavior, especially the presence of multiple cycles and chaos as an example of these studies [22–25]. Two-species nonlinear models without seasonal fluctuations (i.e., constant parameters mode) display only the limit cycle or equilibrium state but become more complex when seasonal fluctuations are assumed. Therefore, it is of great importance in explaining some ecological phenomena, and thus it is taken into account in mathematical models.

There are many studies in the field of theoretical ecology that have addressed the topic of climate impact. In addition, some of them recommended that future efforts should focus on studying the possible effects of climate change on species and ecosystems and evaluating direct and indirect effects, such as [17]. However, in mathematical ecology, less attention has been paid. Although there is a significant lack of mathematical models that examine the impact of climate change on predator-prey interactions, some mathematical models have been proposed in recent studies. Gretkon et al. [26] presented a deterministic model of predator-prey interactions with variable territory and used the carrying capacity and intrinsic growth rate of the prey to incorporate climate change. Sengupta and Das [27] presented a non-autonomous stochastic mathematical model with Holling type-III that incorporates climate and harvest variation for two prey and one predator into the growth rates and carrying capacities of the prey and predators. A spatial gradient was also included using a coupled reaction-diffusion equation for a predator-prey model against the increase in temperature arising from climate change [28]. Sekerci [29] introduced a fractional predator-prey model to study the impact of climate change by considering the predation rate as a function of time. Some deterministic and a stochastic mathematical models were included, including the use of wind speed, seasonality, and global warming to express the effects of climate change, which included modifications to the functional response [30–32]. Recently, Wayesa et al. [33] presented a deterministic model that includes temperature changes due to climate change in reserved and unreserved areas for prey with Holling Type II. The model includes temperature changes as a dynamic change by including a differential equation considering temperature changes in the model.

Significant advances in analytical methods and the development of numerical tools using numerous computer programs have improved our understanding of predator-prey interactions; we refer to some references that include numerical schemes for solving predator-prey models and the mathematical models that contain climate change [34–38].

In contrast to the literature, in this work, we assume that climate change is directly added to the model and has its own term. The primary objective of this study is to start investigating the negative effects of climate change on the dynamics of competitive predator-prey models. These models use Holling types I and II as functional responses. Therefore, the main contribution of this study is to provide predictive scenarios for some of the key dynamics of predator-prey models under the influence of climate change, such as stability, coexistence, and extinction, by using analytical methods and numerical simulations.

According to the following structure, this paper is organized. Section 2 introduces novel models with integrated static climate change. Section 3 addresses the theoretical perspectives of these models, which validate them and study their dynamics, such as stability and the existence of limit cycles, the Hopf bifurcation is introduced, controlled by climate change parameters, proving uniform persistence and obtaining different scenarios of extinction. To verify and explain our theoretical results, numerical simulations are presented in Section 4. In Section 5, the models with forced seasonality to represent periodic climate change are introduced, and they are computationally investigated. Section 6 presents the conclusion of the paper.

2. The proposed of the models with climate static changes

The novel general competitive prey-predator model is proposed with climate change to investigate their long-term effects on the dynamical behaviors. Functional and numerical responses are described by Holling types I and II. Holling type II is the most widely used in numerous theoretical and experimental studies because it is the most realistic, given that there is a handling time when the predator interacts with the prey. However, Holling type I can also be used in certain laboratories or special environments such as filter-feeding crustacean Daphnia pulex preys upon a variety of edible algae. The model without a climate change term has been utilized in prior studies with two and three interacting species to investigate their dynamic behavior for different approaches (see [39–45]). Prey and predator populations are represented by N and P, respectively, to describe their interactions. The general shape of the non-dimensional model is indicated as follows:

$$\frac{dN}{dt} = \zeta N\left(1-\frac{N}{K}\right) - FNP - Q(t)N,$$

$$\frac{dP}{dt} = -\mu P + GNP - GP^2 - Q(t)P. \tag{1}$$

Subject to

$$N(0) = N_0 \geq 0, \quad P(0) = P_0 \geq 0.$$

Where we assume F and G represent functional and numerical responses, respectively, and also, the term $Q(t)$ in model (1) that represents static climate change. So, the models are as follows:

Model 1 The Holling type I predator-prey model with static changes:

$$\frac{dN}{dt} = \zeta N\left(1-\frac{N}{K}\right) - \beta NP - q_1 N = A_1(N, P),$$

$$\frac{dP}{dt} = -\mu P + e\beta NP - e\beta P^2 - q_2 P = A_2(N, P). \tag{2}$$

Model 2 The Holling type II predator-prey model with static changes:

$$\frac{dN}{dt} = \zeta N\left(1-\frac{N}{K}\right) - \frac{\beta NP}{1+h\beta N} - q_1 N = B_1(N, P),$$

$$\frac{dP}{dt} = -\mu P + \frac{e\beta NP}{1+h\beta N} - \frac{e\beta P^2}{1+h\beta N} - q_2 P = B_2(N, P). \tag{3}$$

The systems are subject to positive initial conditions $N(0) = N_0 > 0$ and $P(0) = P_0 > 0$. The biological meanings of the symbols are listed as follows:

- ζ indicates inherent growth rate of prey.
- K represents the system carrying capacity.
- β is the catching rate of the prey by a predator.
- μ is the rate of natural death of predator.
- e is conversion of consumed prey into predators.
- h is the prey handling time.
- q_1 is climate change effects on prey population.
- q_2 is climate change effects on predator population.

The biological significance of the terms and expressions in the models (2) and (3) is clarified as follows:

The logistic term $\zeta N\left(1-\frac{N}{K}\right)$ indicates an intraspecific competition-based growth rate for prey. βNP and $\frac{\beta NP}{1+h\beta N}$ represent predator consumption of prey, which are classified as Holling types I and II functional responses, respectively. In contrast, a change in predator density as a result of prey consumption is indicated by the terms $e\beta NP$ and $\frac{e\beta NP}{1+h\beta N}$, which are classified as Holling types I and II numerical responses, respectively. Predator death rates are expressed in μP. $e\beta P^2$ and $\frac{e\beta P^2}{1+h\beta N}$ indicate intraspecific competition between predators. The terms $q_1 N$ and $q_2 P$ represent static climate change effects on prey and predator populations, respectively. For biological meaning, all parameters are assumed to be positive values; also, $0 \le q_1 \le 1$ and $0 \le q_2 \le 1$.

3. The main analytical results

3.1 *The existence, uniqueness, and positivity*

In this subsection, we will show the existence, uniqueness, and positivity of the solutions of models (2) and (3).

Theorem 3.1 The solutions of models (2) and (3) exist, are unique, and are positive for all values of $t \ge 0$.

We prove the existence, uniqueness, and positivity of model (3), which is a generalization of the model (2), so to avoid repetition of the proofs, the proof of model (2) will be omitted.

Proof. Let

$$\sigma_1(N, P) = \zeta\left(1-\frac{N}{K}\right) - \frac{\beta P}{1+h\beta N} - q_1,$$

$$\sigma_2(N, P) = -\mu + \frac{e\beta N}{1+h\beta N} - \frac{e\beta P}{1+h\beta N} - q_2.$$

Thus, we can reduce the model (3) to:

$$\frac{dN}{dt} = N\sigma_1(N, P), \quad N(0) > 0,$$

$$\frac{dP}{dt} = P\sigma_2(N, P), \quad P(0) > 0. \tag{4}$$

It shows that $N\sigma_1(N, P)$ and $P\sigma_2(N, P)$ are continuous functions of N and P, as well as Lipschitzian functions locally in R_+^2. Therefore, a solution of model (3) exists and is unique on $[0, \vartheta)$, where $0 < \vartheta < \infty$.

According to equation (4), we have

$$\frac{dN}{dt} = N(0)\,exp\left[\int_0^t \sigma_1(N(s), P(s))\right] \geq 0,$$

$$\frac{dP}{dt} = P(0)\,exp\left[\int_0^t \sigma_2(N(s), P(s))\right] \geq 0.$$

Theorem proved. □

3.2 *The boundedness of the models*

In this part, we prove the boundedness of the solution of models (2) and (3).

Theorem 3.2

(i) All the solutions of system (2) that start in R_+^2 for $t \geq 0$ are ultimately bounded.

(ii) All the solutions of system (3) that start in R_+^2 for $t \geq 0$ are ultimately bounded.

We prove the second part, which is a generalization of the first part, so the proof of the first part can be done in the same manner and therefore is omitted.

Proof. For system (3), assume $(N(t), P(t))$ is any solution; we have

$$\frac{dN}{dt} \leq \zeta N\left(1 - \frac{N}{K}\right). \tag{5}$$

The solution of equation (5) is $N(t) = \dfrac{Ke^{t+Kc}}{-1+e^{t+Kc}}$, c is an integration constant. Then

$$\lim_{t\to\infty} \sup N(t) \leq \mathrm{K} \forall t > 0. \tag{6}$$

Now, we show that $N(t) + P(t) \leq \theta$, $\forall t \geq 0$. Consider $\Phi(t) \in C^1(R_+ \to R_+)$ as

$$\Phi(t) = N(t) + P(t) > 0.$$

The derivative of J with respect to time (t) is

$$\frac{d\Phi}{dt} = \frac{dN}{dt} + \frac{dP}{dt}, \tag{7}$$

$$\frac{d\Phi}{dt} = \zeta N\left(1 - \frac{N}{K}\right) - \frac{\beta NP}{1 + h\beta N} - q_1 N - uy + \frac{e\beta NP}{1 + h\beta N} - \frac{e\beta P^2}{1 + h\beta N} - q_2 P. \tag{8}$$

Since $\lim_{t\to\infty} \sup x(t) \le K$, $\max\left\{rx\left(1 - \frac{x}{K}\right)\right\} = \frac{4\zeta}{K}$, then we can assume

$$\frac{d\Phi}{dt} \le \frac{4\zeta}{K} - q_1 N - uP + \frac{e\beta KP}{1 + h\beta N} - \frac{e\beta P^2}{1 + h\beta K} - q_2 P + \Phi - \Phi. \tag{9}$$

The term $\left(1 - q_2 - u + \frac{e\beta K}{1 + h\beta K}\right)P - \frac{e\beta P^2}{1 + h\beta K}$ has a maximum value $\frac{\left(1 - q_2 - u + \frac{e\beta k}{1 + h\beta K}\right)^2 (1 + hK\beta)}{4e\beta} = \xi$, then

$$\frac{d\Phi}{dt} \le \frac{4\zeta}{K} + K + \xi, \tag{10}$$

Let $\vartheta = \frac{4r}{K} + K + \xi$

$$\frac{d\Phi}{dt} + \Phi \le \vartheta. \tag{11}$$

Thus,

$$\Phi(t) \le \vartheta + \Phi(0)e^{-t},$$

for $t \to \infty$, then $\Phi \le \vartheta$. So, J is bounded. As a result, all the solutions of system (3) are contained within

$$\omega = \left\{(N, P) \in R_+^2 : \Phi = \vartheta + \varepsilon\right\}. \tag{12}$$

Thus, the solutions of system (3) are ultimately bounded. □

Remark 3.3 The positivity and boundedness of the solutions in the models validate them biologically.

3.3 *Equilibria, local and global stability analysis*

In this subsection, we show the existence of nonnegative equilibria and study local and global stability. It is noticed that the systems (1) and (2) have three types of equilibrium points for each system that are nonnegative and biologically feasible.

3.3.1 *Equilibria of systems (2) and (3)*

The systems (2) and (3) have three types of equilibrium points for both systems.

• The first type is the trivial equilibrium points, which present the two species going extinct from the system as $E_{0H_I} = E_{0H_{II}} = (N = 0, P = 0)$.

• The second type is the axial equilibrium points that show the coexistence of prey and extinction of predator; the axial equilibrium points of the systems are $E_1 = E_{1H_I} = E_{1H_{II}} = \left(N = \frac{(\zeta - q_1)K}{\zeta}, P = 0\right)$. The axial equilibrium points exist if $\zeta > q_1$.

• The third type is the interior equilibrium points that show the coexistence of both species. For the system (2), we have $E_2 = E_{2H_I} = \left(N = \frac{q_2 K + eK\zeta + K\mu}{\zeta e + eK\beta}, P = \frac{eK\zeta\beta - eKq_1 - \zeta q_2 - \zeta\mu}{\zeta e\beta + eK\beta^2}\right)$. However, for the system (3), we find $\bar{E_2}$ as follows:

$$\bar{E_2} = E_{2H_{II}} = (\bar{N}, \bar{P}),$$

such that we get $\bar{N}$ and $\bar{P}$ through finding the positive root of the following algebraic equations:

$$\zeta\left(1 - \frac{\bar{N}}{K}\right) - \frac{\beta\bar{P}}{1 + h\beta\bar{N}} - q_1 = 0$$

$$-\mu + \frac{e\beta\bar{N}}{1 + h\beta\bar{N}} - \frac{e\beta\bar{P}}{1 + h\beta\bar{N}} - q_2 = 0. \tag{13}$$

We introduce the following analysis to guarantee the feasibility of the interior equilibrium point $\bar{E_2} = E_{2H_{II}} = (\bar{N}, \bar{P})$

$$W(\bar{N}, \bar{P}) = \zeta\left(1 - \frac{\bar{N}}{K}\right) - \frac{\beta\bar{P}}{1 + h\beta\bar{N}} - q_1 = 0. \tag{14}$$

We get from the equation (14):

(i) When $\bar{N} = 0$, then $\bar{P} = \frac{\zeta - q_1}{\beta} = \bar{P}_i$, so $\bar{P}_i > 0$ when $\zeta > q_1$.

(ii) When $\bar{P} = 0$, then $\bar{N} = \frac{K(\zeta - q_1)}{\zeta} = \bar{N}_i$, so $\bar{N}_i > 0$ when $\zeta > q_1$.

(iii)

$$\frac{d\bar{P}}{d\bar{N}} = -\frac{\frac{\partial W}{\partial \bar{N}}}{\frac{\partial W}{\partial \bar{P}}} = \frac{\frac{-\zeta}{K} + \frac{h\beta^2\bar{P}}{(1 + h\beta\bar{N})^2}}{\frac{\beta}{1 + h\beta\bar{N}}}.$$

Consequently, $\frac{d\bar{P}}{d\bar{N}} < 0$ under the following condition:

$$h\beta^2 K\bar{P} < \zeta(1+h\beta\bar{N})^2.$$

We notice from the above analysis that the isocline (14) passes through points $(\bar{N},\,0)$ and $(0,\,\bar{P})$. Also, we have $\bar{P}$ as a decreasing function of $\bar{N}$, if the conditions $\zeta > q_1$ and $h\beta^2 K\bar{P} < \zeta(1+h\beta\bar{N})^2$ are satisfied.

Let

$$Z(\bar{N},\,\bar{P}) = -\mu + \frac{e\beta\bar{N}}{1+h\beta\bar{N}} - \frac{e\beta\bar{P}}{1+h\beta\bar{N}} - q_2 = 0. \tag{15}$$

We get from the equation (15):

(i) When $\bar{N}=0$, then $\bar{P} = \frac{-\mu-q_2}{e\beta} = \bar{P}_{ii}$, so $\bar{P}_{ii} < 0$ always.

(ii) When $\bar{P}=0$, then $\bar{N} = \frac{\mu+q_2}{e\beta-\mu h\beta-q_2 h\beta} = \bar{N}_{ii}$, so $\bar{N} > 0$ when $e > \mu h + q_2 h$.

(iii)

$$\frac{d\bar{P}}{d\bar{N}} = -\frac{\frac{\partial Z}{\partial \bar{N}}}{\frac{\partial Z}{\partial \bar{P}}} = \frac{h\beta\bar{P}+1}{1+h\beta\bar{N}}.$$

Thus, $\frac{d\bar{P}}{d\bar{N}} > 0$ always.

The isocline (15) met the point $(\bar{N}_{ii},\,0)$ with the condition $e > \mu h + q_2 h$; also, the slope is positive.

Based on the above analysis, the two isoclines met at a unique point $\bar{N}$, $\bar{P}$ with the following condition:

$$\bar{N}_{ii} < \bar{N}_i.$$

Figure 1 shows the unique interior equilibrium points of the models (2) and (3), respectively.

For more discussion of the existence of various interior equilibrium points, see for example [46, 47].

Theorem 3.4 The trivial equilibrium points $E_{0H_1} = E_{0H_2} = (0,\,0)$ are locally asymptotically stable if $\zeta < q_1$ and are saddle points if $\zeta > q_1$.

Proof. By replacing $N=0$ and $P=0$, then the Jacobian matrix at $E_{0H_1} = E_{0H_2} = (0,\,0)$ is

$$J(0,\,0) = \begin{bmatrix} \zeta - q_1 & 0 \\ 0 & -\mu - q_2 \end{bmatrix}.$$

The eigenvalues are $\lambda_1 = \zeta - q_1$ and $\lambda_2 = -\mu - q_2$, which clarifies that E_0 is stable if $\zeta < q_1$, but if $\zeta > q_1$, then E_0 is a saddle point because $-\mu - q_2$ is always negative.

□

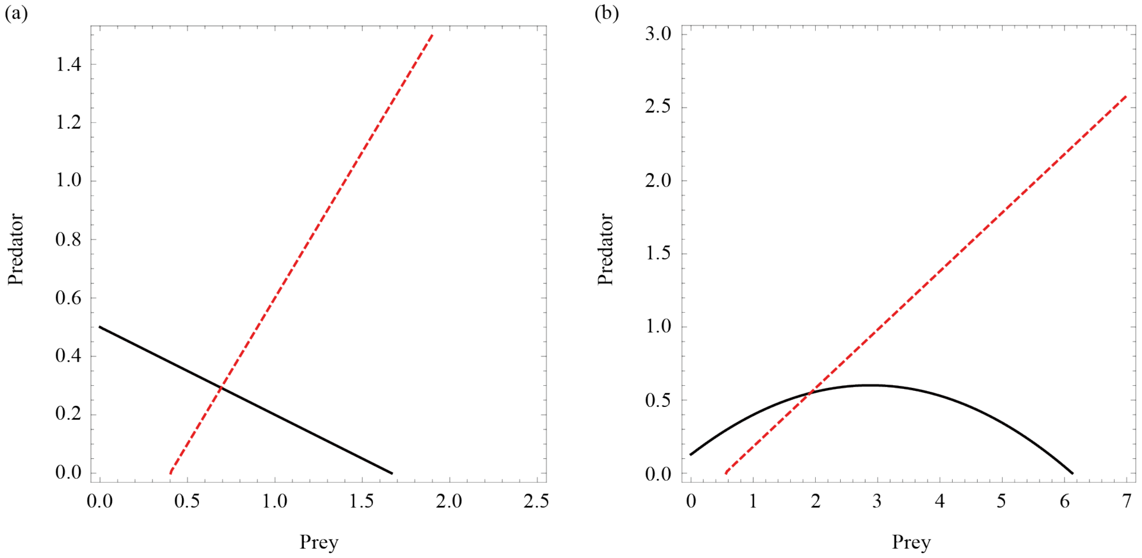

Figure 1. Nullclines of the models (2) and (3), respectively, where the predator nullcline is represented by the red dashed curve and the prey nullcline by the black curve (a) Nullclines for model (2) (i.e., Holling type I). The initial conditions and parameter values are $N(0) = 0.5$, $P(0) = 0.3$, $\zeta = 0.6$, $K = 2$, $\beta = 1.0$, $\mu = 0.1$, $e = 0.5$, $q_1 = 0.1$, $q_2 = 0.1$, (b) Nullclines for model (3) (i.e., Holling type II). The initial conditions and parameter values are $N(0) = 0.5$, $P(0) = 0.3$, $\zeta = 0.8$, $K = 7$, $h = 0.5$, $\beta = 5.5$, $\mu = 0.5$, $e = 0.5$, $q_1 = 0.1$, $q_2 = 0.1$

Theorem 3.5 The axial equilibrium point $E_{1H_I} = \left(N = \dfrac{(\zeta - q_1)K}{\zeta}, P = 0\right)$ is locally asymptotically stable if $\zeta + 2q_1K < 2\zeta K + q_1$ and $\dfrac{e\beta(\zeta - q_1)K}{\zeta} < \mu + q_2$.

Proof. By replacing $N = \dfrac{\zeta K - q_1 K}{\zeta}$ and $P = 0$, then the Jacobian matrix at $E_{1H_I} = \left(N = \dfrac{\zeta K - q_1 K}{\zeta}, P = 0\right)$ is

$$J\left(N = \frac{(\zeta - q_1)K}{\zeta}, 0\right) = \begin{bmatrix} \zeta - 2\zeta K + 2q_1K - q_1 & -\dfrac{\beta K(\zeta - q_1)}{\zeta} \\ 0 & -\mu - q_2 + \dfrac{e\beta(\zeta - q_1)K}{\zeta} \end{bmatrix}.$$

The eigenvalues are $\lambda_1 = \zeta - 2\zeta K + 2q_1K - q_1$ and $\lambda_2 = -\mu - q_2 + \dfrac{e\beta(\zeta - q_1)K}{\zeta}$ that imply the eigenvalues are negative if $\zeta + 2q_1K < 2\zeta K + q_1$ and $\dfrac{e\beta(\zeta - q_1)K}{\zeta} < \mu + q_2$, then E_{1H_I} is locally asymptotically stable. □

Theorem 3.6 The axial equilibrium point $E_{1H_{II}} = \left(N = \dfrac{(\zeta - q_1)K}{\zeta}, P = 0\right)$ is locally asymptotically stable if $\zeta + 2q_1K < 2\zeta K + q_1$ and $\dfrac{e\beta(\zeta - q_1)K}{\zeta + \zeta h\beta(\zeta - q_1)K} < \mu + q_2$.

Proof. By replacing $N = \dfrac{\zeta K - q_1 K}{\zeta}$ and $P = 0$, then the Jacobian matrix at $E_{1H_{II}} = \left(N = \dfrac{\zeta K - q_1 K}{\zeta}, P = 0\right)$ is

$$J\left(N=\frac{(\zeta-q_1)K}{\zeta},0\right)=\begin{bmatrix}\zeta-2\zeta K+2q_1K-q_1 & -\dfrac{\beta K(\zeta-q_1)}{\zeta+h\beta\zeta(\zeta-q_1)}\\ 0 & -\mu-q_2+\dfrac{e\beta(\zeta-q_1)K}{\zeta+\zeta h\beta(\zeta-q_1)K}\end{bmatrix}.$$

The eigenvalues are $\lambda_1=\zeta-2\zeta K+2q_1K-q_1$ and $\lambda_2=-\mu-q_2+\dfrac{e\beta(\zeta-q_1)K}{\zeta+\zeta h\beta(\zeta-q_1)K}$ that imply the eigenvalues are negative if $\zeta+2q_1K<2\zeta K+q_1$ and $\dfrac{e\beta(\zeta-q_1)K}{\zeta+\zeta h\beta(\zeta-q_1)K}<\mu+q_2$, then $E_{1H_{II}}$ is locally asymptotically stable. □

Theorem 3.7 In R_+^2, the interior equilibrium point E_{2H_I} is globally asymptotically stable whenever it exists.

Proof. Suppose $F(x,y)=\dfrac{1}{NP}$ is a Dulac function, which is smooth in R_+^2. Let $L_1(N,P)=\dfrac{dN}{dt}$ and $L_2(N,P)=\dfrac{dP}{dt}$. Now, the Dulac function is multiplied by the prey equation of system (2) and the partial derivatives are taken according to N, which gives:

$$FL_1=\frac{1}{NP}\left(\zeta N\left(1-\frac{N}{k}\right)-\beta NP-q_1N\right)$$

$$FL_1=\frac{1}{P}\left(\zeta-\frac{\zeta N}{K}\right)-\frac{1}{NP}\beta NP+\frac{1}{NP}q_1N$$

$$FL_1=\frac{\zeta}{P}-\frac{\zeta N}{KP}-\beta-\frac{q_1}{P}\tag{16}$$

$$\frac{\partial FL_1}{\partial N}=-\frac{\zeta}{KP}\tag{17}$$

In the same manner, the Dulac function is multiplied by the predator equation of system (2), and taking the partial derivatives according to P, we get:

$$FL_2=\frac{1}{NP}(-\mu P+e\beta NP-e\beta P^2-q_2P)$$

$$FL_2=\frac{-\mu P}{NP}+\frac{e\beta NP}{NP}-\frac{e\beta P^2}{NP}-\frac{q_2P}{NP}$$

$$FL_2=\frac{-\mu}{N}+e\beta-\frac{e\beta P}{N}-\frac{q_2}{N}\tag{18}$$

$$\frac{\partial FL_2}{\partial P}=-\frac{e\beta}{N}$$

Thus,

$$\Delta(FL_1, FL_2) = \frac{\partial FL_1}{\partial N} + \frac{\partial FL_2}{\partial P} = -\frac{\zeta}{KP} - \frac{e\beta}{N} < 0. \tag{19}$$

$\Delta(FN_1, FN_2)$ is always negative and is not identically zero in R_+^2, since $N > 0$, $P > 0$, and all parameters are positive. Therefore, by the Poincare-Bendixson theorem, the interior equilibrium point E_{2H_I} is globally asymptotically stable. □

Theorem 3.8 There is no periodic solution of the system (2) in R_+^2.

Proof. Since the system (2) is globally asymptotically stable in R_+^2 whenever the interior equilibrium point exists, and using the Bendixson-Dulac criterion, the system (2) does not have a periodic solution. □

Theorem 3.9 The interior equilibrium point $E_{2H_{II}} = (\bar{N}, \bar{P})$ is locally asymptotically stable if the following conditions are satisfied:

$$\zeta - \frac{2\zeta\bar{N}}{K} - \frac{\beta\bar{P}}{(1+h\beta\bar{P})^2} - q_1 < 0, \tag{20}$$

$$-\mu - q_2 + \frac{e\beta(\bar{N} - 2\bar{P})}{1+h\beta\bar{N}} < 0. \tag{21}$$

Proof. The Jacobian matrix of the system (3) when substituting the interior equilibrium point $E_{2H_{II}}$ is obtained as follows:

$$J(\bar{N}, \bar{P}) = \begin{bmatrix} \zeta - \dfrac{2\zeta\bar{N}}{K} - \dfrac{\beta\bar{P}}{(1+h\beta\bar{N})^2} - q_1 & \dfrac{-\beta\bar{N}}{1+h\beta\bar{N}} \\[2ex] \dfrac{e\beta\bar{P}(1+h\beta\bar{P})}{(1+h\beta\bar{N})^2} & -\mu - q_2 + \dfrac{e\beta(\bar{N}-2\bar{P})}{1+h\beta\bar{N}} \end{bmatrix},$$

which can be rewritten as follows:

$$J(\bar{N}, \bar{P}) = \begin{bmatrix} c_{11} & -c_{12} \\ c_{21} & c_{22} \end{bmatrix},$$

where

$$c_{11} = \zeta - \frac{2\zeta\bar{N}}{K} - \frac{\beta\bar{P}}{(1+h\beta\bar{N})^2} - q_1,$$

$$c_{12} = \frac{\beta\bar{N}}{1+h\beta\bar{N}},$$

$$c_{21} = \frac{e\beta\bar{P}(1+h\beta\bar{P})}{(1+h\beta\bar{N})^2},$$

$$c_{22} = -\mu - q_2 + \frac{e\beta(\bar{N} - 2\bar{P})}{1 + h\beta\bar{N}}.$$

Since $c_{12} < 0$ and $c_{21} > 0$, we have $|J(\bar{N}, \bar{P})| > 0$ and $Trace\big(J(\bar{N}, \bar{P})\big) < 0$, if $c_{11} < 0$ and $c_{22} < 0$. Therefore, the interior equilibrium point $E_{2H_{II}} = (\bar{N}, \bar{P})$ with the conditions is locally asymptotically stable (20) and (21). □

Theorem 3.10 In R^2_+, the system (3) possesses periodic dynamics.

Proof. To prove the theorem, let $T(N, P) = \frac{1}{NP}$ be a smooth Dulac function in R^2_+.

Suppose $S_1(N, P) = \frac{dN}{dt}$ and $S_2(N, P) = \frac{dP}{dt}$. The Dulac function is multiplied by the prey equation of system (3), and the partial derivatives with respect to N are computed, yielding:

$$GS_1 = \frac{1}{NP}\left(\zeta N\left(1 - \frac{N}{k}\right) - \frac{\beta NP}{1 + h\beta N} - q_1 N\right)$$

$$GS_1 = \frac{1}{P}\left(\zeta\left(1 - \frac{N}{k}\right) - \frac{\alpha P}{1 + h\beta N} - q_1\right)$$

$$GS_1 = \frac{\zeta}{P} - \frac{\zeta N}{KP} - \frac{\beta}{1 + h\beta P} - \frac{q_1}{P} \tag{22}$$

$$\frac{\partial GS_1}{\partial N} = -\frac{\zeta}{KP} + \frac{h\beta^2}{(1 + h\beta N)^2} \tag{23}$$

Also, taking the partial derivatives of P from the Dulac function multiplied by the predator equation of system (3) results in:

$$GS_2 = \frac{1}{NP}\left(-\mu P + \frac{e\beta NP}{1 + h\alpha N} - \frac{e\beta}{1 + h\alpha N}P^2\right)$$

$$GS_2 = \frac{-\mu}{N} + \frac{e\beta}{1 + h\beta N} - \frac{e\beta P}{N(1 + h\beta N)} \tag{24}$$

$$\frac{\partial GS_2}{\partial P} = -\frac{e\alpha}{N(1 + h\beta N)}$$

Thus,

$$\Delta(GS_1, GS_2) = \frac{\partial GS_1}{\partial N} + \frac{\partial GS_2}{\partial P} = -\frac{\zeta}{KP} + \frac{h\beta^2}{(1 + h\beta N)^2} - \frac{e\alpha}{N(1 + h\beta N)} \tag{25}$$

Given that $N > 0$ and $P > 0$, along with all parameters being positive, it follows that $\Delta(GS_1, GS_2)$ changes sign and is non-zero in R^2_+. Since the system (3) is bounded from Theorem 3.2 and utilizing the Poincare-Bendixson theorem, the system (3) has periodic dynamics. □

3.4 *Hopf bifurcation*

A Hopf bifurcation occurs when a system loses stability and transitions to a periodic solution as certain parameters change. This subsection analyzes the Hopf bifurcation at the interior equilibrium point. The system (2) is globally stable, as demonstrated by Theorem 3.7, so there is no bifurcation under any conditions. However, the internal point $E_{2H_{II}}$ of the system (3) can be stable or unstable. To investigate the Hopf bifurcation, we use q_1 and q_2 as bifurcation parameters, which are the factors of climate change.

Theorem 3.11 System (3) exhibits a Hopf bifurcation around the internal equilibrium point ($E_{2H_{II}} = (\bar{N}, \bar{P})$) at the threshold $q_1 = q_{1H}$, where $q_{1H} = \zeta - \frac{2\zeta\bar{N}}{K} - \frac{\beta\bar{P}}{(1+h\beta\bar{P})^2}$.

Proof. If $q_1 > q_{1H}$, then $q = q_{1H}$ is the critical value where the stability of $E_{2H_{II}} = (\bar{N}, \bar{P})$ changes; the internal equilibrium point $E_{2H_{II}} = (\bar{N}, \bar{P})$ will be unstable in this case.

Suppose that $\lambda = A(m) + B(m)i$ is an eigenvalue in the Jacobian matrix $J((\bar{N}, \bar{P}); q_{1H}))$. Thus, λ is a purely imaginary number, and when $q = q_{1H}$, there is a Hopf bifurcation. We verify these conditions by substituting q_1 with q_{1H}, we obtain that

$Trace(J((\bar{N}, \bar{P}); q_{1H})) = 0$, $Det(J((\bar{N}, \bar{P}); q_{1H})) > 0$ and $\frac{d(trace(J((\bar{N}, \bar{P}); q_{1H})))}{dq_1} = -1 \neq 0$. Thus, a Hopf bifurcation occurs at the point $q_1 = q_{1H}$. □

Theorem 3.12 System (3) exhibits a Hopf bifurcation around the internal equilibrium point ($E_{2H_{II}} = (\bar{N}, \bar{P})$) at the threshold $q_2 = q_{2H}$, where $q_{2H} = -\mu + \frac{e\beta(\bar{N} - 2\bar{P})}{1 + h\beta\bar{N}}$.

Proof. The proof is similar to Theorem 3.12. □

3.5 *Persistence and extinction scenarios*

In this part, we present a theoretical analysis to infer the conditions of persistence and extinction. Consider the following notation: $\lim_{t\to\infty} \sup P(t) = \tilde{P}$.

Theorem 3.13 The system (3) is uniformly persistent under the following condition:

$$e\beta K > \mu + \mu h\beta K. \tag{26}$$

Proof. Let the average Lyapunov function be:

$$\Lambda(N, P) = N^{S_1} P^{S_2}, \ (N, P) \in R^2_+, \tag{27}$$

where $\Lambda_i > 0$, for $i = 1, 2$. The function Λ_i represents a continuously differentiable non-negative function. The differentiation of equation (27) with regard to t is as follows:

$$\frac{\dot{\Lambda}}{\Lambda} = S_1\frac{\dot{N}}{N} + S_2\frac{\dot{P}}{P}, \tag{28}$$

$$\Psi = S_1\left\{\zeta\left(1 - \frac{N}{K}\right) - \frac{\beta P}{1 + h\beta N} - q_1\right\} + S_2\left\{-\mu + \frac{e\beta N}{1 + h\beta N}\right\}, \tag{29}$$

$$\Psi(0,\,0) = S_1(\zeta - q_1) + S_2(-\mu - q_2). \tag{30}$$

Assuming that

$$\zeta > q_1, \tag{31}$$

it follows that $\Psi(0,\,0) > 0$ for some $S_1,\, S_2 > 0$.

$$\Psi(K,\,0) = q_2\left\{-\mu + \frac{e\beta K}{1 + \beta h K}\right\}, \tag{32}$$

S_1 and S_2 are chosen so that $\Psi(0,\,0) > 0$. Also, $\Psi(K,\,0) > 0$, if the following condition is satisfied

$$e\beta K > \mu + \mu h\beta K.$$

As a result, system (3) is uniformly persistent under the condition (26). □

Remark Destabilization of boundary equilibrium points implies persistence.

Because Holling type II is more general than the Holling type I, the coexistence condition for the system (2) is deduced, which is stated in the following theorem:

Theorem 3.14 When the following condition is met, the system (2) is uniformly persistent:

$$e\beta K > \mu. \tag{33}$$

Theorem 3.15 Under the following condition:

$$\zeta < q_1, \tag{34}$$

the prey population goes extinct from systems (2) and (3) in the long term.

Proof.

$$\frac{dN}{dt} = \zeta N \left(1 - \frac{N}{K}\right) - \frac{\beta NP}{1 + h\beta N} - q_1 N \leq \zeta N - \frac{\beta NP}{1 + h\beta N} - q_1 N,$$

$$< (\zeta - q_1) N,$$

$$= -I_1 N, \quad \text{where} \quad I_1 = q_1 - \zeta > 0.$$

Therefore,

$$\lim_{t \to \infty} N(t) = 0.$$

This completes the proof. □

Theorem 3.16 For the systems (2) and (3), the prey species go extinct with time under the following condition:

$$\zeta < q_1 + \beta \tilde{P}. \tag{35}$$

Proof. Select δ such that $0 < \delta < \tilde{P} - \frac{\zeta - q_1}{\beta}$. If $\forall t > T$, then $\exists\, T > 0$ such that $P(t) > \tilde{P} - \delta$.

$$\frac{dN}{dt} = \zeta N \left(1 - \frac{N}{K}\right) - \frac{\beta NP}{1 + h\beta N} - q_1 N \leq \zeta N - \beta NP - q_1 N,$$

$$< \left(\zeta - \beta(\tilde{P} - \delta) - q_1\right) N,$$

$$= -I_2 N, \forall t > T \quad \text{where} \quad I_2 = q_1 + \beta(\tilde{P} - \delta) - \zeta > 0.$$

Therefore,

$$\lim_{t \to \infty} N(t) = 0.$$

This completes the proof. □

Theorem 3.17 In the systems (2) and (3), the predator species dies out with time under the following condition:

$$e\beta K < \mu. \tag{36}$$

Proof.

$$\frac{dP}{dt} = -\mu P + \frac{e\beta NP}{1+h\beta N} - \frac{e\beta P^2}{1+h\beta N} - q_2 P,$$

$$\leq -\mu P + \frac{e\beta NP}{1+h\beta N},$$

$$< -\mu P + e\beta PN.$$

From Equ (6), $\lim_{t\to\infty} \sup N(t) \leq \mathrm{K} \forall t > 0$, we get

$$< (-\mu + e\beta K) P,$$

$$= -I_3 P, \forall t > T \quad \text{where} \quad I_3 = \mu - e\beta K > 0.$$

Therefore,

$$\lim_{t\to\infty} P(t) = 0.$$

This completes the proof. □

Theorem 3.18 In the systems (2) and (3), the predator species dies out with time under the following condition:

$$e\beta K < \mu + q_2. \tag{37}$$

Proof. Select δ such that $0 < \delta < \tilde{P} - \frac{\zeta - q_1}{\beta}$. If $\forall t > T$, then $\exists\, T > 0$ such that $P(t) > \tilde{P} - \delta$.

$$\frac{dP}{dt} = -\mu P + \frac{e\beta NP}{1+h\beta N} - \frac{e\beta P^2}{1+h\beta N} - q_2 P,$$

$$\leq -\mu P + \frac{e\beta NP}{1+h\beta N} - q_2 P,$$

$$< -\mu P + e\beta PN - q_2 P.$$

From Equ (6), $\lim_{t\to\infty} \sup N(t) \leq K \forall t > 0$, we get

$$Z < (-\mu + e\beta K - q_2)P,$$

$$= -I_4 P, \forall t > T \quad \text{where} \quad I_4 = \mu + q_2 - e\beta K > 0.$$

Therefore,

$$\lim_{t \to \infty} P(t) = 0.$$

This completes the proof. □

Remark 3.19 The previous analysis in Subsections 3.2 and 3.3 shows that negative climate impacts play an important role in system stability, as well as in the coexistence and extinction of species exposed to these impacts. Consequently, species' biological systems may adapt, their density may decline, or they may become extinct over time, depending on the severity of these impacts.

4. Numerical simulations

In this section, we show several numerical simulations to verify and visualize our analytical results that are presented in Section 3. The Mathematica software package is utilized to perform numerical simulations that display the impacts of negative climate change on dynamical behaviors. The numerical simulations are executed using the "NDSOLVE" command, and then they are plotted. For more details, see Wolfram's website [48]. The initial conditions for all numerical simulations are assumed as follows:

$$N(0) = 0.5, \; P(0) = 0.3. \tag{38}$$

4.1 *Numerical simulations for Holling type I*

In this part, the results are shown for the model with Holling Type 1. The system (2) has been shown to be globally stable without conditions (i.e., Theorem 3.7). The parameter values are assumed to satisfy Theorem 3.14, which means that the species persist. On the other hand, we show the effects of climate change on the persistence and extinction of species. The first set of parameter values is selected as follows:

$$\zeta = 0.6, \; K = 2, \; \beta = 1.0, \; \mu = 0.1, \; e = 0.5. \tag{39}$$

With the free effects of climate change, Figure 2 illustrates that the dynamic behavior of the model (2) persists stably around the equilibrium point (0.615, 0.415). This is consistent with condition (33) of Theorem 3.14. Figure 3 depicts model (2) with $(q_1 = 0.1, \; q_2 = 0.1)$, which indicates equal and minor effects of climate change on prey and predators. The dynamic behavior of the model (2) remains stable near the equilibrium point (0.692, 0.292), as shown in Figure 3. This meets condition (33) of Theorem 3.14. However, when assuming the existence of small enough effects of climate change on the prey population and high enough effects of climate change on the predator population (that is, $q_1 = 0.1$, $q_2 = 0.8$) of the model (2), Figure 4 explains that there is an extinction of the predator population and an increase of the prey population but will not reach carrying capacity without the threat from the predator population to be around the equilibrium point

(1.667, 0.0), which is a consequence of climate change. This satisfies condition (37) of Theorem 3.18. On the other hand, Figure 5 shows that the system has collapsed for prey and predator populations when the effects of climate change are high in the prey population and small enough in the predator population. In line with condition (35) of Theorem 3.16, the extinction of the prey population leads to the extinction of the predator population, despite the small effects of climate change on the predator population, resulting in the collapse of the predator-prey system.

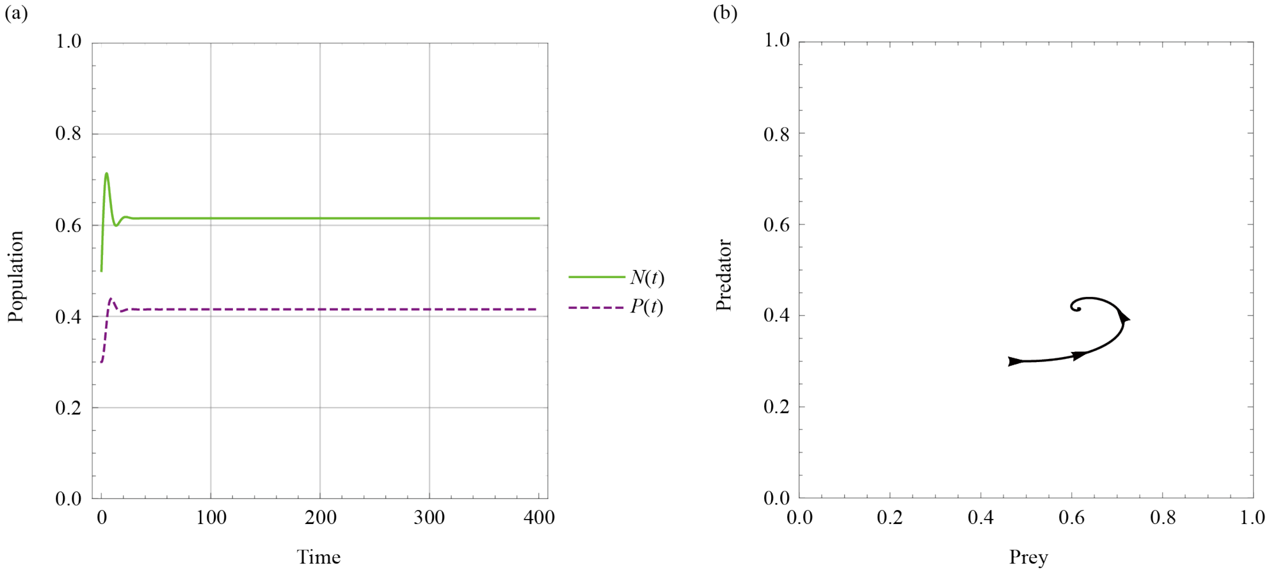

Figure 2. Dynamics of the model (2) with free climate change effects on prey and predator populations (i.e., $q_1 = 0.0$, $q_2 = 0.0$), which shows they persist stably around the equilibrium point (0.615, 0.415): (a) Time series, (b) Phase portrait trajectories. The first set of other parameter values (39) is used

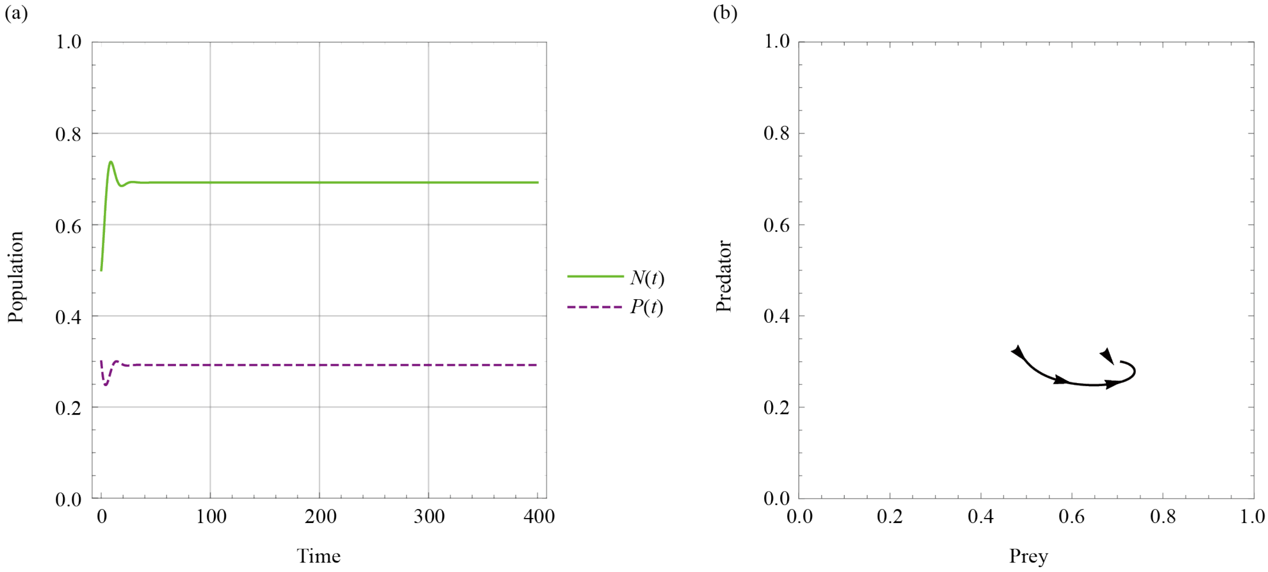

Figure 3. Dynamics of the model (2) with equal and small enough effects of climate change on prey and predator populations (i.e., $q_1 = 0.1$, $q_2 = 0.1$), which shows they persist stably around the equilibrium point (0.692, 0.292): (a) Time series, (b) Phase portrait trajectories. The first set of other parameter values (39) is used

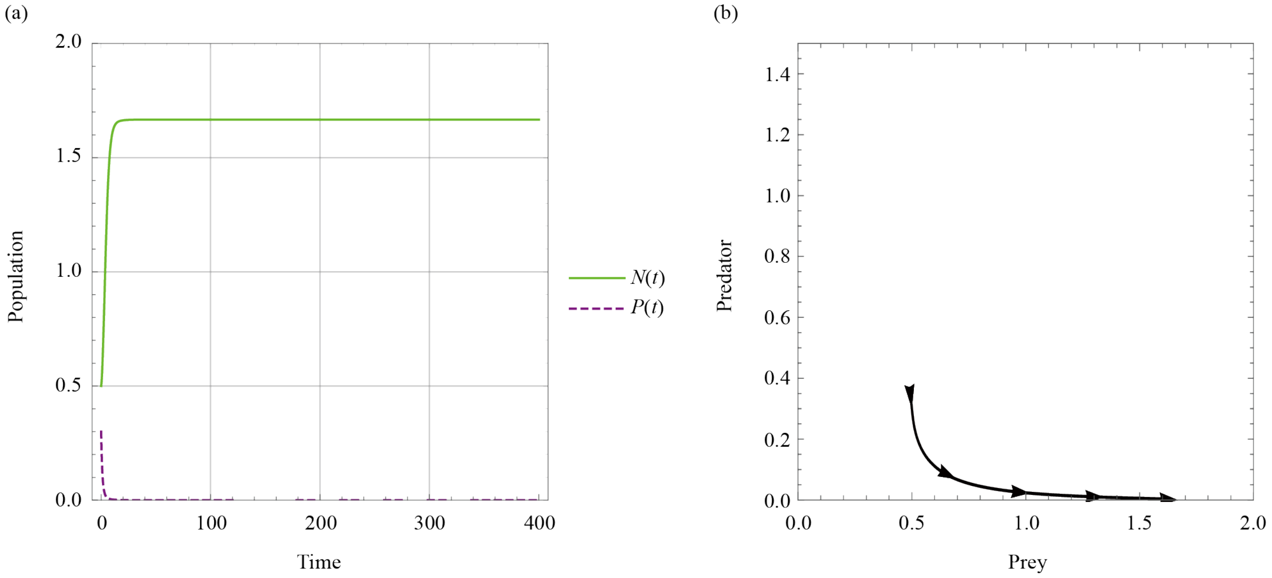

Figure 4. Dynamics of the model (2) with small enough effects of climate change on the prey population and high enough effects of climate change on the predator population (i.e., $q_1 = 0.1$, $q_2 = 0.8$), which shows prey population persists and predator population extincts around the equilibrium point (1.667, 0.0): (a) Time series, (b) Phase portrait trajectories. The first set of other parameter values (39) is used

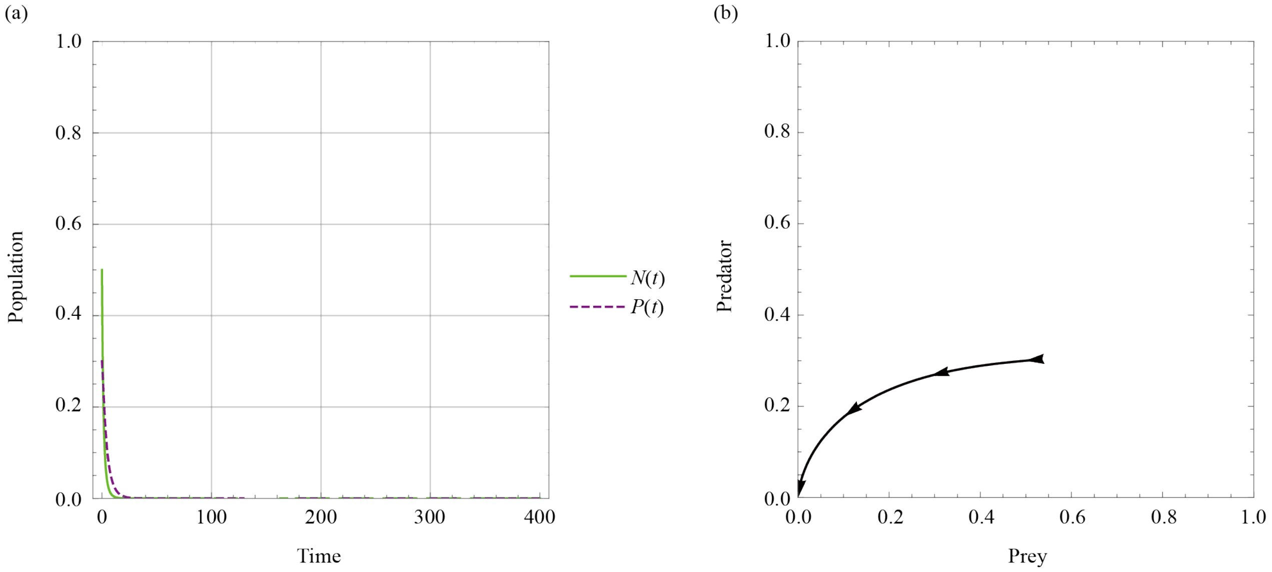

Figure 5. Dynamics of the model (2) with high enough effects of climate change on the prey population and small enough effects of climate change on the predator population (i.e., $q_1 = 0.8$, $q_2 = 0.1$), which shows collapse of the predator-prey system: (a) Time series, (b) Phase portrait trajectories. The first set of other parameter values (39) is used

4.2 *Numerical simulations for Holling type II*

The dynamic behaviors with Holling type II of the model (3) are analytically explained in Section 3, which presents two different dynamics: steady state and limit cycle, as shown through Theorems 3.9 and 3.10. Here, the effects of climate change on the limit cycle of the dynamical shape of the model (3) are investigated. The second set of parameter values is selected to satisfy Theorems 3.10 and 3.13, which means that the species periodically persists. The second set of parameter values is selected to investigate the dynamics as follows:

$$\zeta = 0.8,\ K = 7,\ \beta = 5.5,\ h = 0.5,\ \mu = 0.5,\ e = 0.5. \tag{40}$$

Remark 4.1 In this subsection, the persistence of steady-state dynamic behavior is not shown numerically because it shows similar figures as presented in subsection 4.1.

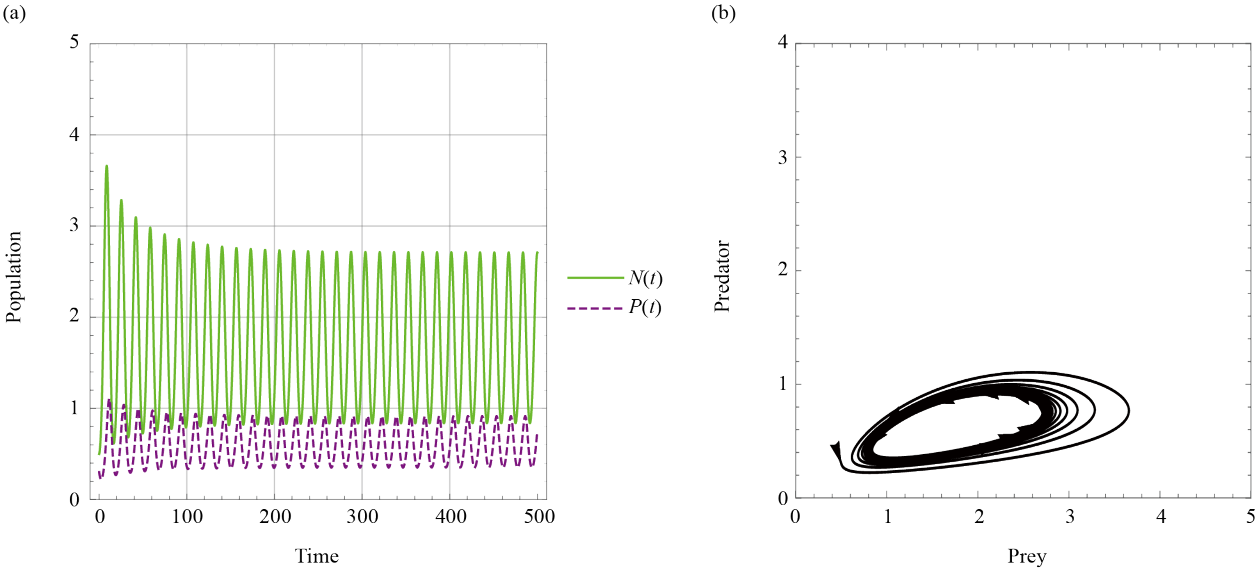

Figure 6. Dynamics of the model (3) with free climate change effects on prey and predator populations (i.e., $q_1 = 0.0$, $q_2 = 0.0$), which shows they persist in a limit cycle: (a) Time series, (b) Phase portrait trajectories. The second set of other parameter values (40) is used

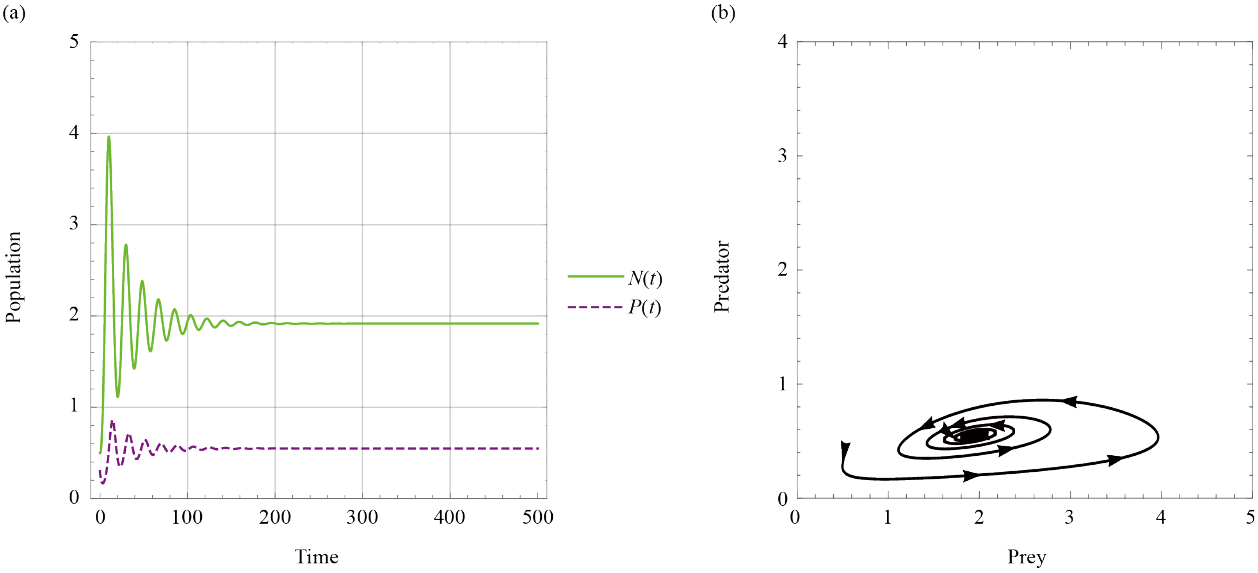

Figure 7. Dynamics of the model (3) with equal and small enough effects of climate change on prey and predator populations (i.e., $q_1 = 0.1$, $q_2 = 0.1$), which shows they persist stably around the equilibrium point (1.916, 0.548): (a) Time series, (b) Phase portrait trajectories. The second set of other parameter values (40) is used

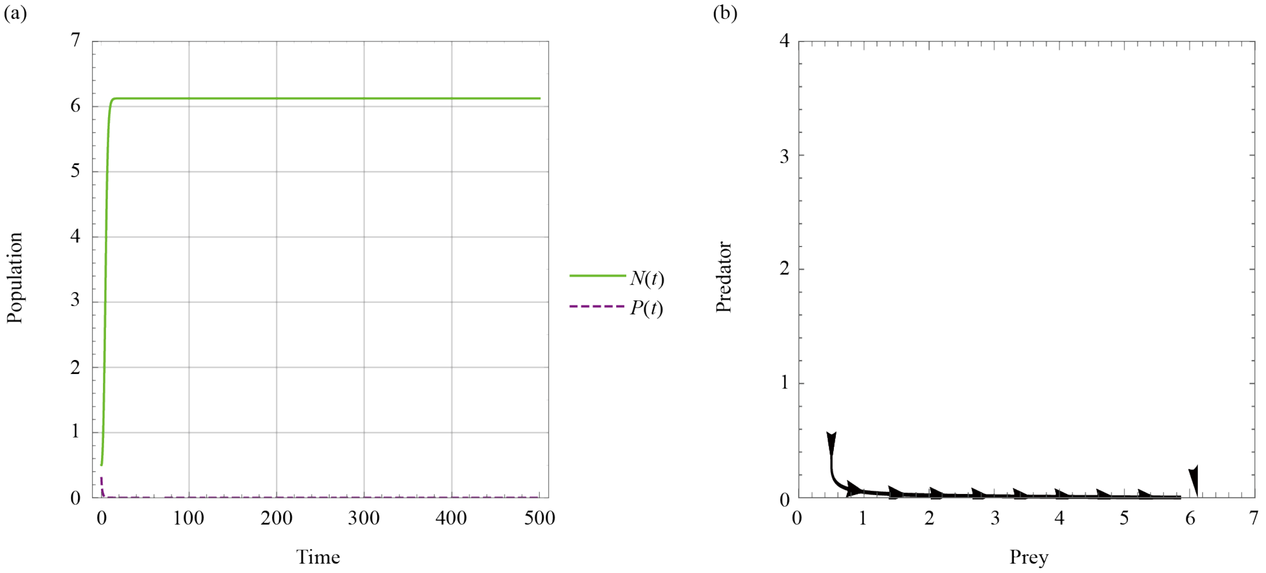

Figure 8. Dynamics of the model (3) with small enough effects of climate change on the prey population and high enough effects of climate change on the predator population (i.e., $q_1 = 0.1$, $q_2 = 0.8$), which shows prey population persists and predator population extincts around the equilibrium point (6.125, 0.0): (a) Time series, (b) Phase portrait trajectories. The second set of other parameter values (40) is used

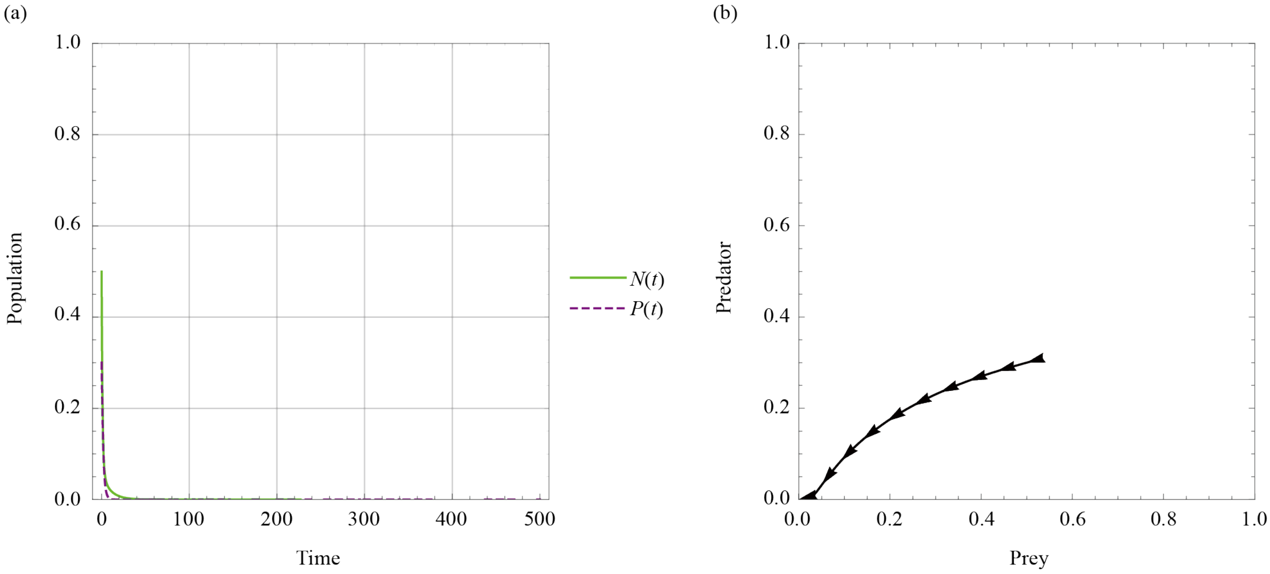

Figure 9. Dynamics of the model (3) with high enough effects of climate change on the prey population and small enough effects of climate change on the predator population (i.e., $q_1 = 0.8$, $q_2 = 0.1$), which shows collapse of the predator-prey system: (a) Time series, (b) Phase portrait trajectories. The second set of other parameter values (40) is used

With free climate change effects, Figure 6 shows limit cycle dynamical behavior, and both populations persist, which satisfies the conditions of Theorems 3.16 and 3.17. However, when assuming $(q_1 = 0.1,\ q_2 = 0.1)$, which means that the same and small effects of climate change hold on the prey and predator populations, Figure 7 shows that the dynamical behavior of the system (3) appears that the dynamics have shifted significantly to become a steady coexisting state around the equilibrium point (1.916, 0.548). This satisfies the condition (26) of Theorem 3.13. This result may be ecologically interpreted as the adaptation of a predator-prey system with these effects or the existence of other factors such as the existence of prey refuge, and it can persist stably even with lower prey and predator density. However, when assuming the existence of small enough effects of climate change on the prey population and high enough effects of climate change on the predator population ($i.e.$, $q_1 = 0.1$, $q_2 = 0.8$) of the model (3), Figure 8 explains that there is an extinction of the predator population and an increase in the prey population, but it will not reach carrying capacity with no threat from the predator population around the equilibrium point (6.125, 0.0); this is due to impacts of climate change. As shown in Figure 9, the predator and prey populations have collapsed. According to Theorem 3.5, condition (34) shows that there is an extinction of prey populations, resulting in the extinction of predator populations and the collapse of prey-predator systems.

We summarize the results in the following Table 1:

Table 1. Description of Dynamical behavior for all cases

Values of climate change (q_1 and q_2)	Dynamical behavior for every species		Other notes
	The model with Holling type I (i.e., Model (2))		
	Prey	Predator	
$q_1 = 0.0$ and $q_2 = 0.0$ (Figure 2)	Persist (steady state)	Persist (steady state)	The equilibrium point is (0.615, 0.415)
$q_1 = 0.1$ and $q_2 = 0.1$ (Figure 3)	Persist (steady state)	Persist (steady state)	The equilibrium point is (0.692, 0.292)
$q_1 = 0.1$ and $q_2 = 0.8$ (Figure 4)	Persist (steady state)	Extinct	The equilibrium point is (1.667, 0.0)
$q_1 = 0.8$ and $q_2 = 0.1$ (Figure 5)	Extinct	Extinct	-
	The model with Holling type II (i.e., Model (3))		
$q_1 = 0.0$ and $q_2 = 0.0$ (Figure 6)	Persist (limit cycle)	Persist (limit cycle)	-
$q_1 = 0.1$ and $q_2 = 0.1$ (Figure 7)	Persist (steady state)	Persist (steady state)	Change the dynamics from limit cycle to steady state around the equilibrium point (1.916, 0.548)
$q_1 = 0.1$ and $q_2 = 0.8$ (Figure 8)	Persist (steady state)	Extinct	The equilibrium point is (6.125, 0.0)
$q_1 = 0.8$ and $q_2 = 0.1$ (Figure 9)	Extinct	Extinct	-

Remark 4.2 Some ecological justifications for the reasons behind extinction can be explained as follows:

Extinction may occur due to a shift from habitat to a more suitable one (i.e., migration from the environment) or due to extreme events such as floods or forest fires, which may wipe out some or all species.

Remark 4.3 Real-world examples are given as follows:

Our results can be explained by relying on some real-world examples, such as the following: As polar bears prey on seals, it was indicated that polar bears are a threatened species in the Arctic Ocean due to climate change and global warming, which could disrupt the natural balance, as Sengupta and Das [49] indicated from "World Wildlife". Another real-world example is the impact of windy conditions on lions' predation on springbok and zebra species more frequently than on wildebeest [50].

5. Climate change effects with forced seasonality

One concrete evidence of climate change is the presence of seasonal changes over relatively short periods of time, which may help scientists understand the evolution of impacts of climate change over longer periods of time. The climatic effects on seasonality include their strength, frequency, and duration, and therefore there is a strong correlation between climate change and seasonality [51]. The study of environmental variability is very important for population communities, which may explain many of the dynamic changes in these communities. Some studies have been presented in this area, which have clarified the effect of seasonality on the predator-prey system, for instance [24, 52, 53]. Therefore, we integrate the model (1) with forced seasonality terms as periodic climate change impacts by including a sinusoidal function. Since Holling types I and II are used as functional responses, two models are formed as follows:

Model 3 Holling type I prey-predator model with seasonality effects (periodic changes through time):

$$\frac{dN}{dt} = \zeta N\left(1-\frac{N}{K}\right) - \beta NP - q_1(1+(\nu\sin(wt)))N = A_1(N, P),$$

$$\frac{dP}{dt} = -\mu P + e\beta NP - e\beta P^2 - q_2(1+(\nu\sin(wt)))P = A_2(N, P). \tag{41}$$

Model 4 Holling type II prey-predator model with seasonality effects (periodic changes over time):

$$\frac{dN}{dt} = \zeta N\left(1-\frac{N}{K}\right) - \frac{\beta NP}{1+h\beta N} - q_1(1+(\nu\sin(wt)))N = B_1(N, P),$$

$$\frac{dP}{dt} = -\mu P + \frac{e\beta NP}{1+h\beta N} - \frac{e\beta P^2}{1+h\beta N} - q_2(1+(\nu\sin(wt)))P = B_2(N, P), \tag{42}$$

where ν indicates the degree of seasonality strength and w represents angular frequency and subjects the systems to initial conditions $N(0) = N_0 > 0$ and $P(0) = P_0 > 0$.

In this section, we computationally investigate the impacts of periodic climate change on the dynamical behavior of the models (41) and (42) by performing several numerical simulations. It has been shown in section 3 that the dynamics are in two forms: at the limit cycle or in a stable state. In contrast, ecological communities in nature exhibit extremely complex dynamic behaviors. Mathematically, seasonality contributes to the manifestation of complex dynamic destabilization states, such as multiple cycles and chaos cases, as indicated in some studies. Instability cases can increase the risk of species extinction.

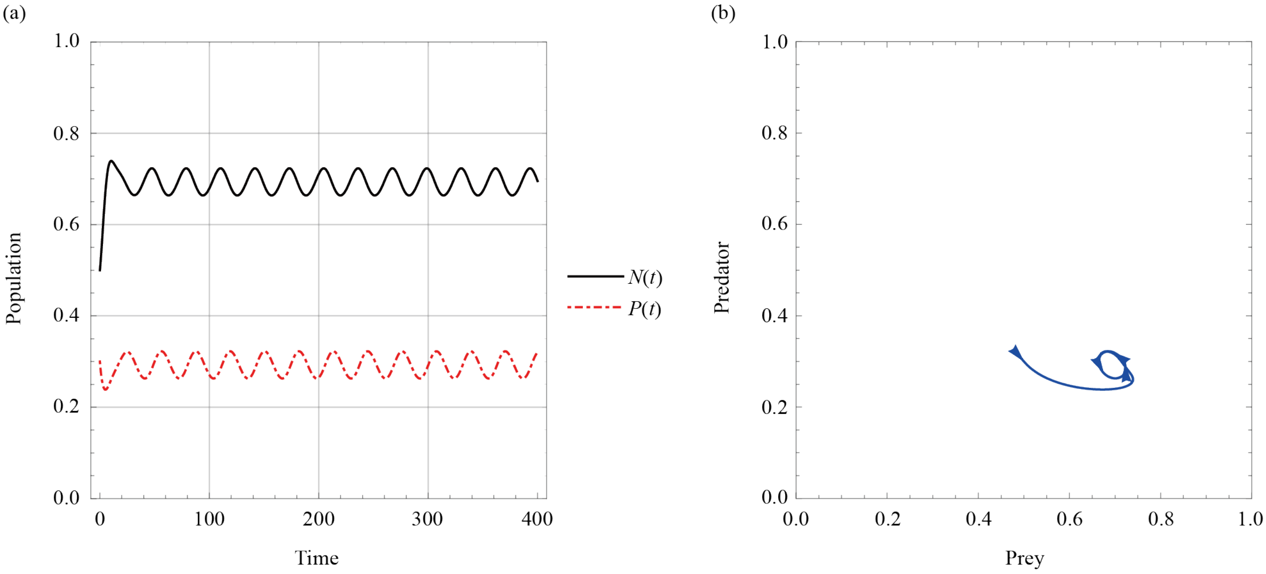

Figure 10. Dynamics of the model (41) with forcing small enough seasonality (i.e., $\nu = 0.2$), which shows both populations persist in a limit cycle with small cycle size: (a) Time series, (b) Phase portrait trajectories. The first set of other parameter values (39) and the value of $w = 0.2$ are used

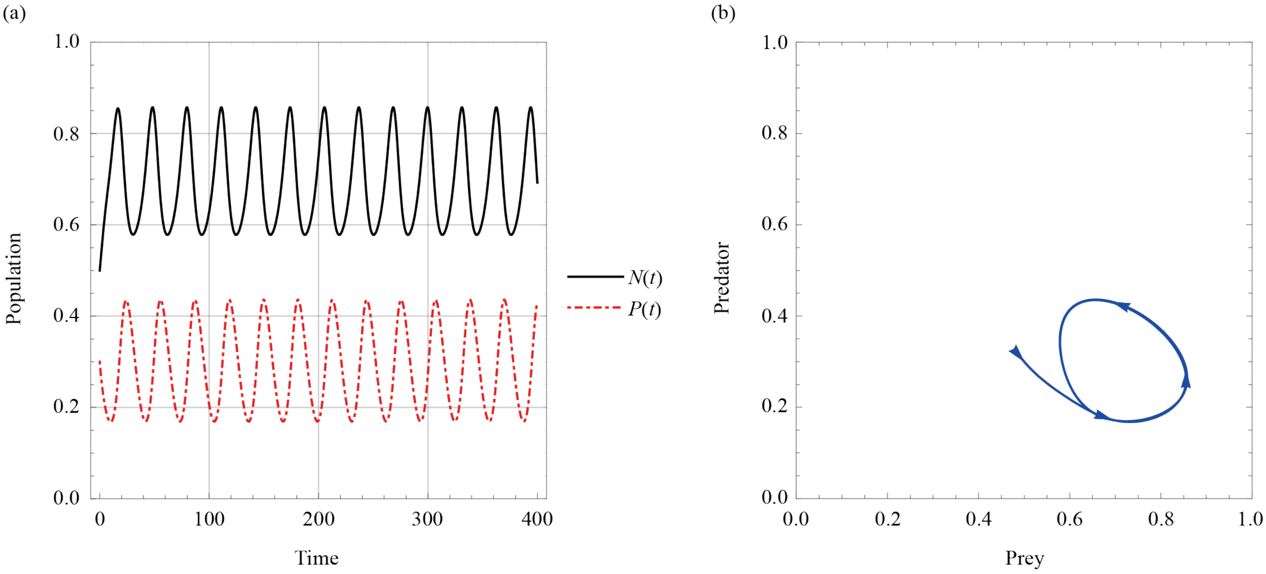

Figure 11. Dynamics of the model (41) with forcing high enough seasonality (i.e. $\nu = 0.9$), which shows both populations persist in a limit cycle with big cycle size: (a) Time series, (b) Phase portrait trajectories. The first set of other parameter values (39) and the value of $w = 0.2$ are used

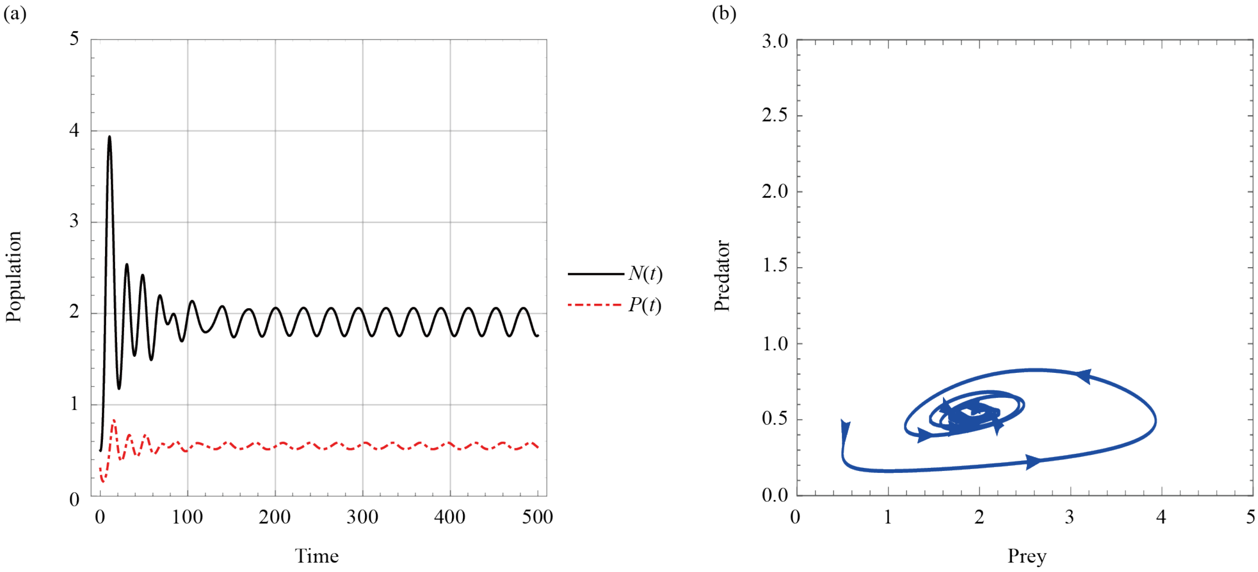

Figure 12. Dynamics of the model (42) with forcing small enough seasonality (i.e. $\nu = 0.2$), which shows both populations persist in a limit cycle with big cycle size: (a) Time series, (b) Phase portrait trajectories. The second set of other parameter values (40) and the value of $w = 0.2$ are used

The initial conditions values are the same as those used in the set (38) for all figures. In models (41) and (42) and for Figures 10-13, we use the same values as the sets (39) and (40), respectively, as well as the value of $w = 0.2$ that it does not have in models (2) and (3). It is assumed that the impacts of climate change are equally affected on prey and predator populations at $q_1 = 0.1$ and $q_2 = 0.1$, which satisfies the persistence conditions (33) and (26) of Theorems 3.13 and 3.14, respectively, when assuming free seasonality effects; this is shown in Figure 3. In addition, the parameter ν that does not appear in models (2) and (3), is a pivotal parameter to study the effect of periodic climate change, so the value of ν is varied in the range $[0, 1]$ for each case. However, the system (41) shows a significant shift in the dynamics of the system to become a limit cycle when introducing seasonality effects by setting $\nu = 0.2$, as shown in Figure 10. In addition, when increasing the strength of seasonality by setting $v = 0.9$, the system (41) displays a limit cycle with increasing the size of the cycle that approaches the axes, which indicates an increase in the probability of species extinction, as shown in Figure 11.

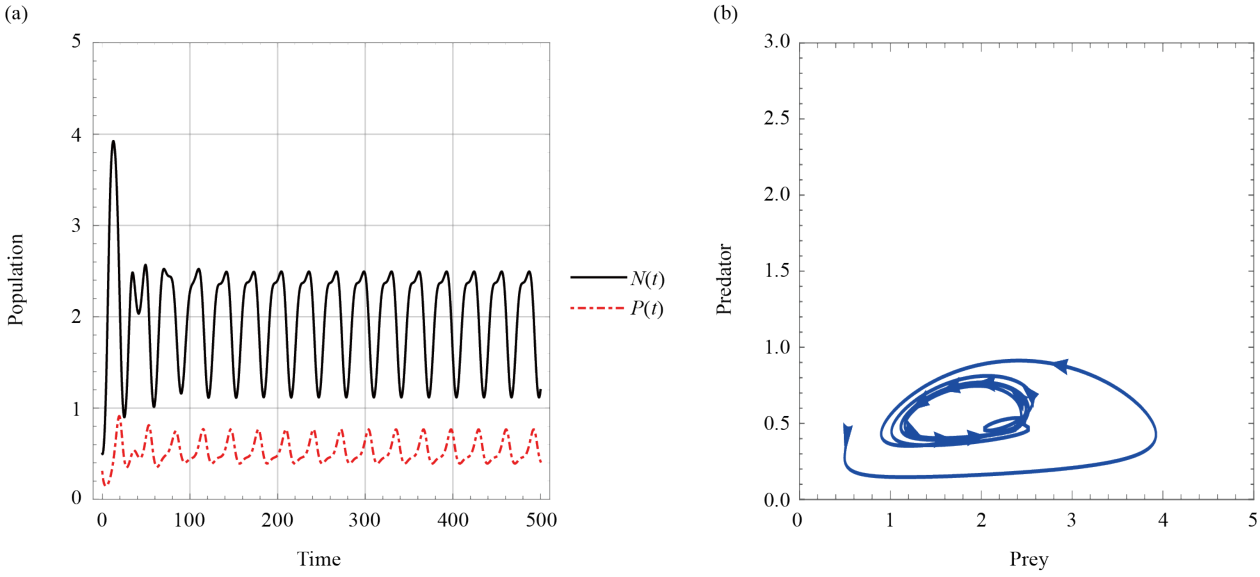

Figure 13. Dynamics of the model (42) with forcing high enough seasonality (i.e. $v = 0.9$), which shows both populations persist in a limit cycle with big cycle size: (b) Time series, (b) Phase portrait trajectories. The second set of other parameter values (40) and the value of $w = 0.2$ are used

In the system (42) with the second set (40), it was observed that there was an important shift in the dynamic behavior when the impact of climate change was assumed as shown previously through in Figure 7. However, when introducing seasonality effects by setting $v = 0.2$, the dynamic behavior becomes destabilized, as shown in Figure 12. Also, the destabilization state increases with increasing the strength of seasonality by setting $v = 0.9$, as illustrated in Figure 13.

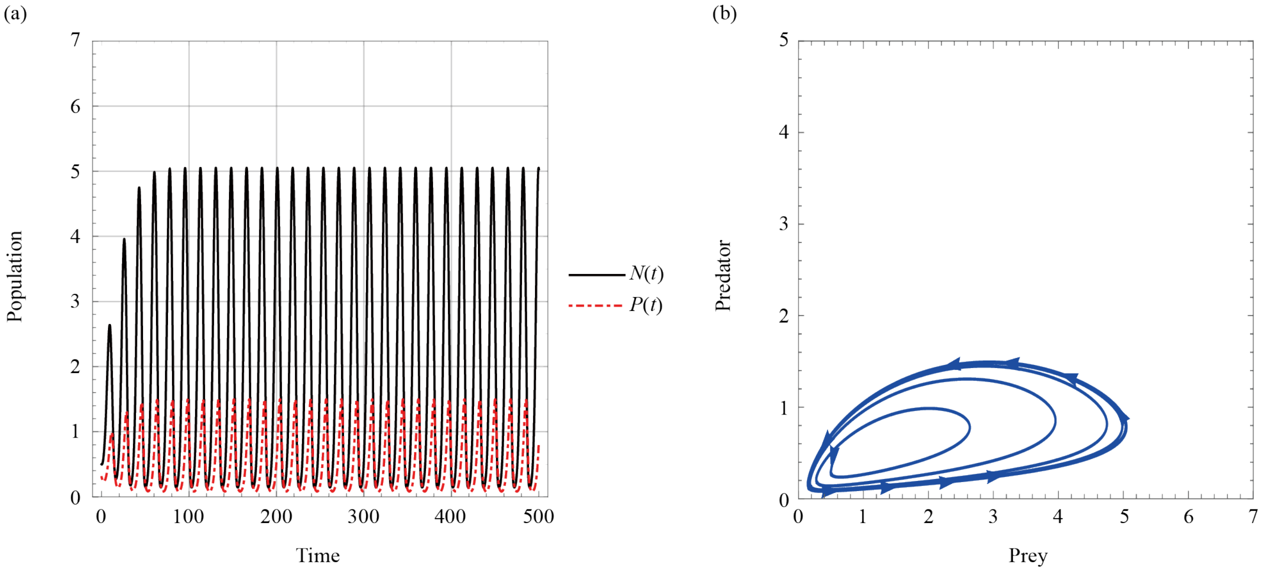

Figure 14. Dynamics of the model (42) with free forcing seasonality (i.e. $v = 0.0$), which shows both populations persist in a limit cycle: (a) Time series, (b) Phase portrait trajectories. The third set of other parameter values (43) and the value of $w = 0.2$ are used

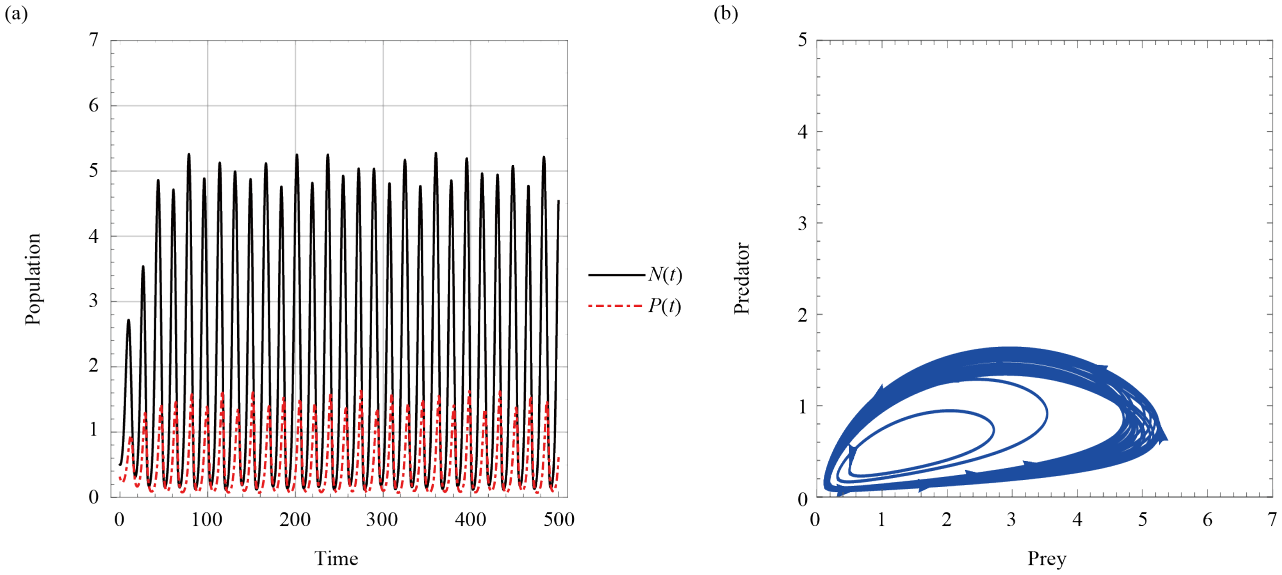

Figure 15. Dynamics of the model (42) with forcing small enough seasonality (i.e., $\nu = 0.2$), which shows both populations persist in multiple cycles: (a) Time series, (b) Phase portrait trajectories. The third set of other parameter values (43) and the value of $w = 0.2$ are used

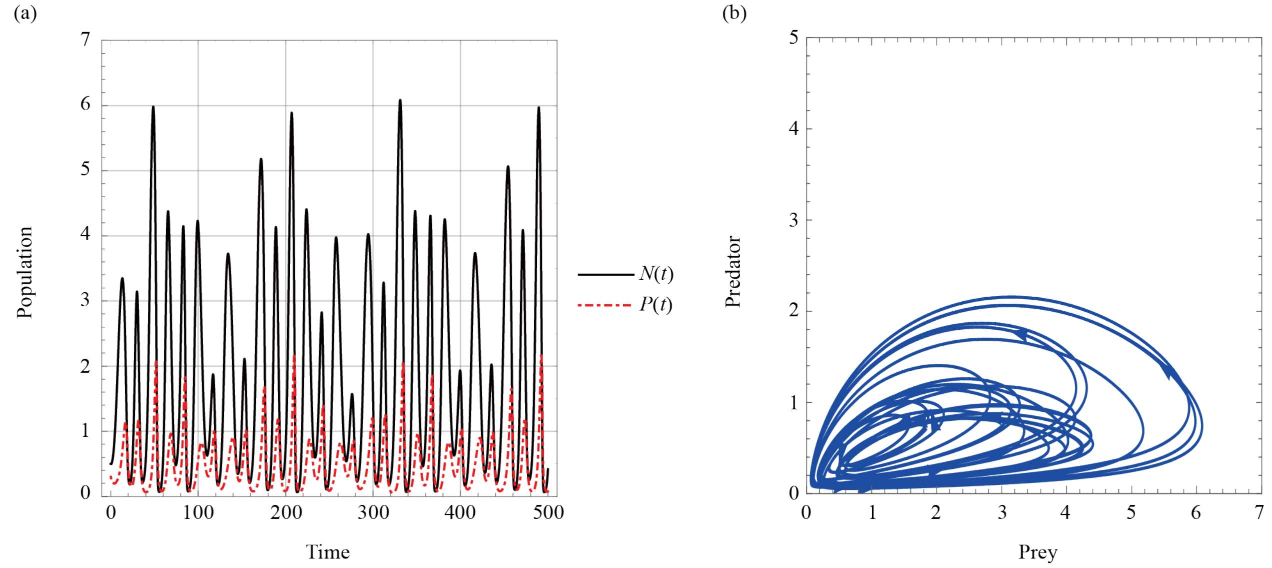

Figure 16. Dynamics of the model (42) with forcing high enough seasonality (i.e., $\nu = 0.9$), which shows both populations persist in chaos: (a) Time series, (b) Phase portrait trajectories. The third set of other parameter values (43) and the value of $w = 0.2$ are used

Figures 14-16 display the impact of seasonality effects with the existence of climate changes on the dynamics of prey and predator populations in the persistence destabilization state of the model (42), when assuming free seasonality effects (i.e., $\nu = 0.0$), this is consistent with Theorems 3.10 and 3.13, so the third set of parameter values is specified as follows:

$$\zeta = 1.0,\ K = 10,\ \beta = 7.5,\ h = 0.5,\ \mu = 0.25,\ e = 0.5,\ q_1 = 0.1,\ q_2 = 0.1,\ w = 0.2. \tag{43}$$

The values of ν are taken to be small enough ($\nu = 0.2$) and high enough ($\nu = 0.9$) for seasonality strength. Figure 14 shows the dynamics of the system (42) with free seasonality ($\nu = 0.0$) as a limit cycle. However, when introducing the seasonality, the dynamics become more complex with multiple cycles when the seasonality strength is small enough ($\nu = 0.2$), as shown in Figure 15, and the dynamics become chaotic behavior when the seasonality strength is high enough ($\nu = 0.9$), as shown in Figure 16.

We summarize the results in the following Table 2:

Table 2. Description of Dynamical behavior for all cases

Values of seasonality intensity (ν)	Dynamical behavior for every species		Other notes
	The model with Holling type I (i.e., Model (41))		
	Prey	Predator	
$\nu = 0$ (Figure 3)	Persist (steady state)	Persist (steady state)	The equilibrium point is (0.692, 0.292)
$\nu = 0.2$ (Figure 10)	Persist (limit cycle)	Persist (limit cycle)	Small size of limit cycle
$\nu = 0.9$ (Figure 11)	Persist (limit cycle)	Persist (limit cycle)	Big size of limit cycle
	The model with Holling type II (i.e., Model (42))		
$\nu = 0$ (Figure 7)	Persist (steady state)	Persist (steady state)	Change the dynamics from limit cycle to steady state around the equilibrium point (1.916, 0.548)
$\nu = 0.2$ (Figure 12)	Persist (limit cycle)	Persist (limit cycle)	Small size of limit cycle
$\nu = 0.9$ (Figure 13)	Persist (limit cycle)	Persist (limit cycle)	Big size of limit cycle
	The model with Holling type II (i.e., Model (42))		
$\nu = 0$ (Figure 14)	Persist (limit cycle)	Persist (limit cycle)	-
$\nu = 0.2$ (Figure 15)	Persist (multiple cycles)	Persist (multiple cycles)	-
$\nu = 0.9$ (Figure 16)	Persist (chaos)	Persist (chaos)	-

Remark 5.1 Some ecological justifications for multiple cycles and chaos dynamics can be explained as follows:

The Didinium-Paramecium predator-prey system is a standard laboratory tool for studying predator-prey dynamics. [54] investigated how temperature affects this system, altering the shape of the cycles. In this context, [53] stated that one possible reason for the emergence of multiple cycles and chaos dynamics is the overpredation of prey species; this can be inferred by considering seasonality within the system, which serves as concrete evidence of climate change.

Remark 5.2 Conservation strategies can be presented:

There are some strategies that can be offered to mitigate the negative effects of climate change and preserve species, such as increasing shelters, increasing nature reserves, preserving species through the rescue phenomenon, and other strategies that may be future work in this direction.

6. Conclusions

In this paper, we examine a significant issue: the negative impact of climate change on predator-prey interactions. Novel model is presented that directly includes negative climate change. This effect is modeled by assuming a negative term so that the value of the climate change factor is between zero and one (i.e., $0 \leq q_1, q_2 \leq 1$), thus having a biological meaning. Our argument is also based on describing the impact of climate change as both constant and periodic changes. This involves using the seasonality assumption in climate change factors, as seasonality and fluctuations are inherently linked to climate change and may encompass extreme events. Thus, the effect includes migration, extinction, or even adaptation to climate change. Holling types of functional responses I and II are used in these models due to their wide use in predator-prey models.

For constant changes, the existence, uniqueness, positivity, and boundedness of the solutions of these models have been shown to be biologically valid, as presented in Theorems 3.1 and 3.2. Feasible equilibrium points have been obtained and their stability studied, which shows that the model with Holling type I (i.e., model (2)) is globally stable whenever an internal equilibrium point exists, but the model with Holling type II (i.e., model (3)) displays two dynamic behaviors: stable and limit cycle states, as shown in Theorems 3.4-3.10. The Hopf bifurcation is examined, by taking climate change constants, as bifurcation parameters. In addition, uniform persistence is proved, and different scenarios of extinction have been obtained using theoretical analysis, as shown in subsection 3.5. The theoretical results have been numerically verified. Negative climate changes are shown to play an important role in extinction when climate change is large enough. However, in one case, as shown in Figure 7, it is shown that if climate change is small enough, it can be a stabilizing factor, which can be explained by the appearance of adaptations of predator-prey interactions to these changes [12] or through the presence of other factors, such as the presence of refuge for prey [55, 56], either harvesting the prey species, predator species, or both [57], or wind speed [31] that have stabilizing effects on these systems and prevent extinction.

Periodic changes have been examined numerically but in a different way in which the climate change factor is fixed and the seasonal intensity is assumed to be variable, which shows a greater diversity in dynamic behavior compared with static models. Dynamical behaviors include multiple cycles and chaotic states. The diversity of dynamics due to seasonality forced is compatible with the literature, as shown in [58–62].

In our study, numerous undesirable scenarios for predator-prey interactions were identified, including extinction and complex dynamics that lead to chaotic states, which cannot be predicted later due to negative climate change. However, other scenarios were shown that are capable of reaching states of stability and surviving predator-prey interactions with less severe negative climate change and lower population densities. Therefore, more research can be conducted in future work to obtain scenarios that help preserve biodiversity and species and stabilize ecosystems in the face of adverse climate change.

Acknowledgement

The author extends the appreciation to the Deanship of Postgraduate Studies and Scientific Research at Majmaah University for funding this research work through the project number (R-2025-1740).

Conflict of interest

The author declares no competing financial interest.

References

[1] Lotka AJ. *Elements of Physical Biology*. Maryland, USA: Williams & Wilkins; 1925.
[2] Volterra V. *Variazioni e Fluttuazioni del Numero d'individui in Specie Animali Conviventi [Variations and Fluctuations in the Number of Individuals in Coexisting Animal Species]*. Rome, Italy: Società Anonima Tipografica Leonardo da Vinci; 1926.
[3] Leslie PH. Some further notes on the use of matrices in population mathematics. *Biometrika*. 1948; 35(3/4): 213-245.
[4] Holling CS. Some characteristics of simple types of predation and parasitism. *The Canadian Entomologist*. 1959; 91(7): 385-398.
[5] Rosenzweig ML, MacArthur RH. Graphical representation and stability conditions of predator-prey interactions. *The American Naturalist*. 1963; 97(895): 209-223.

[6] Hassell MP, Varley GC. New inductive population model for insect parasites and its bearing on biological control. *Nature*. 1969; 223: 1133-1137.

[7] May RM. Limit cycles in predator-prey communities. *Science*. 1972; 177(4052): 900-902.

[8] Maynard-Smith J. *Models in Ecology. CUP Archive*. London: Cambride University Press; 1978.

[9] Freedman HI. *Deterministic Mathematical Models in Population Ecology*. New York: Marcel Dekker Inc.; 1980.

[10] Kuang Y. Basic properties of mathematical population models. *International Journal of Biomathematics*. 2002; 17(2): 129-142.

[11] Alebraheem J, Abu-Hassan Y. A novel mechanism measurement of predator interference in predator-prey models. *Journal of Mathematical Biology*. 2023; 86: 84.

[12] DeMarche ML, Doak DF, Morris WF. Incorporating local adaptation intoforecasts of species' distribution and abundance under climate change. *Global Change Biology*. 2019; 25(3): 775-793.

[13] Nunez S, Arets E, Alkemade R, Verwer C, Leemans R. Assessing the impacts of climate change on biodiversity: is below 2 °C enough. *Climatic Change*. 2019; 154: 351-365.

[14] Robertson BA, Rehage JS, Sih A. Ecological novelty and the emergence of evolutionary traps. *Trends in Ecology & Evolution*. 2013; 28(9): 552-560.

[15] Zimova M, Mills LS, Nowak JJ. High fitness costs of climate change-induced camouflage mismatch. *Ecology Letters*. 2016; 19(3): 299-307.

[16] Vucic-Pestic O, Ehnes RB, Rall BC, Brose U. Warming up the system: higher predator feeding rates but lower energetic efficiencies. *Global Change Biology*. 2011; 17(3): 1301-1310.

[17] Bastille-Rousseau G, Schaefer JA, Peers MJ, Ellington EH, Mumma MA, Rayl ND, et al. Climate change can alter predator-prey dynamics and population viability of prey. *Oecologia*. 2018; 186(3): 141-150.

[18] Mondal N, Alrabaiah H, Barman D, Roy J, Alam S. Influence of predator incited fear and interference competition in the dynamics of prey-predator system where the prey species are protected in a reserved area. *Ecology Environment and Conservation*. 2022; 28(2): 831-852.

[19] Morin A, Chamaillé-Jammes S, Valeix M. Climate effects on prey vulnerability modify expectations of predator responses to short-and long-term climate fluctuations. *Frontiers in Ecology and Evolution*. 2021; 28: 601202.

[20] Walther GR, Post E, Convey P, Menzel A, Parmesan C, Beebee TJ, et al. Ecological responses to recent climate change. *Nature*. 2002; 416(6879): 389-395.

[21] Dell AI, Pawar S, Savage VM. Temperature dependence of trophic interactions are driven by asymmetry of species responses and foraging strategy. *Journal of Animal Ecology*. 2014; 83(1): 70-84.

[22] Upadhyay RK, Iyengar S. Effect of seasonality on the dynamics of 2 and 3 species prey-predator systems. *Nonlinear Analysis: Real World Applications*. 2005; 6(3): 509-530.

[23] Yu H, Zhao M. Seasonally perturbed prey-predator ecological system with the beddington-deangelis functional response. *Discrete Dynamics in Nature and Society*. 2012; 2012(1): 150359.

[24] Sauve AM, Taylor RA, Barraquand F. The effect of seasonal strength and abruptness on predator-prey dynamics. *Journal of Theoretical Biology*. 2020; 491: 110175.

[25] Barman D, Naskar S, Mandal A, Alam S. Impact of seasonal variability of sea waves on the dynamics of a predator-prey system. *The European Physical Journal Plus*. 2023; 138(7): 641.

[26] Gretchko S, Marley J, Tyson RC. The effects of climate change on predator-prey dynamics. *arXiv:180511816*. 2018. Available from: https://doi.org/10.48550/arXiv.1805.11816.

[27] Sengupta S, Das P. Dynamics of two-prey one-predator non-autonomous type-III stochastic model with effect of climate change and harvesting. *Nonlinear Dynamics*. 2019; 97: 2777-2798.

[28] Sekerci Y. Climate change effects on fractional order prey-predator model. *Chaos, Solitons & Fractals*. 2020; 134: 109690.

[29] Sekerci Y. Adaptation of species as response to climate change: Predator-prey mathematical model. *AIMS Mathematics*. 2020; 5(4): 3875-3898.

[30] Barman D, Roy J, Alam S. Impact of wind in the dynamics of prey-predator interactions. *Mathematics and Computers in Simulation*. 2022; 191: 49-81.

[31] Barman D, Upadhyay RK. Modelling predator-prey interactions: a trade-off between seasonality and wind speed. *Mathematics*. 2023; 11(23): 4863.

[32] Thirthar AA, Jawad S, Majeed SJ, Nisar KS. Impact of wind flow and global warming in the dynamics of prey-predator model. *Results in Control and Optimization*. 2024; 15: 100424.

[33] Wayesa NN, Obsu LL, Dawed MY. Analysis of predator-prey model with inclusion of temperature variability in prey refugees. *Journal of Applied Mathematics*. 2024; 2024(1): 5138320.

[34] Ejaz A, Nawaz Y, Arif MS, Mashat DS, Abodayeh K. Stability analysis of predator-prey system with consuming resource and disease in predator species. *CMES-Computer Modeling in Engineering & Sciences*. 2022; 132(2): 489-506.

[35] Arif MS, Abodayeh K, Nawaz Y. A computational approach to a mathematical model of climate change using heat sources and diffusion. *Civil Engineering Journal*. 2022; 8(7): 1358-1368.

[36] Arif MS, Abodayeh K, Ejaz A. On the stability of the diffusive and non-diffusive predator-prey system with consuming resources and disease in prey species. *Mathematical Biosciences and Engineering*. 2023; 20(3): 5066-5093.

[37] Arif MS, Abodayeh K, Ejaz A. Stability analysis of fractional-order predator-prey system with consuming food resource. *Axioms*. 2023; 12(1): 64.

[38] Arif MS, Abodayeh K, Nawaz Y. Numerical schemes for fractional energy balance model of climate change with diffusion effects. *Emerging Science Journal*. 2023; 7(3): 808-820.

[39] Alebraheem J, Abu-Hasan Y. Persistence of predators in a two predators-one prey model with non-periodic solution. *Applied Mathematical Sciences*. 2012; 6(19): 943-956.

[40] Alebraheem J, Abu-Hasan Y. Dynamics of a two predator-one prey system. *Computational and Applied Mathematics*. 2014; 33(19): 767-780.

[41] Alebraheem J. Relationship between the paradox of enrichment and the dynamics of persistence and extinction in prey-predator systems. *Symmetry*. 2018; 10(10): 532.

[42] Toaha S, Yusrianto, Kasbawati. Stability analysis of prey predator model with Holling II functional response and threshold harvesting for the predator. *Journal of Physics: Conference Series*. 2019; 1341(6): 062025.

[43] Castillo-Alvino H, Marvá M. The competition model with Holling type II competitive response to interfering time. *Journal of Biological Dynamics*. 2020; 14(1): 222-244.

[44] Arif GE, Alebraheem J, Yahia WB. Dynamics of predator-prey model under fluctuation rescue effect. *Baghdad Science Journal*. 2023; 20(5): 1741-1750.

[45] Alebraheem J, Ibrahim TQ, Arif GE, Hamdi AA, Bazighifan O, Ali AH. The stabilizing effect of small prey immigration on competitive predator-prey dynamics. *Mathematical and Computer Modelling of Dynamical Systems*. 2024; 30(1): 605-625.

[46] Vishwakarma K, Sen M. Influence of Allee effect in prey and hunting cooperation in predator with Holling type-III functional response. *Journal of Applied Mathematics and Computing*. 2022; 68: 249-269.

[47] Vishwakarma K. Dynamics of a predator-prey model with maturation delay and hunting cooperation in predator. *International Journal of Applied and Computational Mathematics*. 2025; 11(2): 1-25.

[48] *Introduction to Advanced Numerical Differential Equation Solving in the Wolfram Language*. Wolfram; 2025 [Accessed 2nd April 2025].

[49] Sengupta S, Das P. Dynamics of two-prey one-predator non-autonomous type-III stochastic model with effect of climate change and harvesting. *Nonlinear Dynamics*. 2019; 97: 2777-2798.

[50] Stander PE, Albon SD. Hunting success of lions in a semi-arid environment. In: *Symposia of the Zoological Society of London*. Oxford: Oxford Academic; 1993. p.127-143.

[51] McCarthy JJ. *Climate Change 2001: Impacts, Adaptation, and Vulnerability: Contribution of Working Group II to the Third Assessment Report of the Intergovernmental Panel on Climate Change*. London: Cambridge University Press; 2001.

[52] Alebraheem J. Dynamics of a predator-prey model with the effect of oscillation of immigration of the prey. *Diversity*. 2021; 13(1): 23.

[53] Barman D, Upadhyay RK. Modelling predator-prey interactions: A trade-off between seasonality and wind speed. *Mathematics*. 2023; 11(23): 4863.

[54] DeLong JP, Lyon S. Temperature alters the shape of predator-prey cycles through effects on underlying mechanisms. *PeerJ*. 2020; 8: e9377.

[55] Kar TK. Stability analysis of a prey-predator model incorporating a prey refuge. *Communications in Nonlinear Science and Numerical Simulation*. 2005; 10(6): 681-691.

[56] Yue Q. Dynamics of a modified Leslie-Gower predator-prey model with Holling-type II schemes and a prey refuge. *SpringerPlus*. 2016; 5: 461.

[57] Belew B, Melese D. Modeling and analysis of predator-prey model with fear effect in prey and hunting cooperation among predators and harvesting. *Journal of Applied Mathematics*. 2022; 2022(1): 2776698.

[58] Gakkhar S, Naji RK. Seasonally perturbed prey-predator system with predator-dependent functional response. *Chaos, Solitons & Fractals*. 2003; 18(5): 1075-1083.

[59] Yu H, Zhao M. Seasonally perturbed prey-predator ecological system with the beddington-deangelis functional response. *Chaos, Solitons & Fractals*. 2012; 2012(1): 150359.

[60] Alebraheem J, Hasan YA. Effects the strength of seasonality on persistence and extinction in prey predator models. *AIP Conference Proceedings*. 2014; 1605(1): 191-196.

[61] Bhargava M, Dubey B. Trade-off dynamics and chaotic behavior in nonautonomous prey-predator model with group defense. *Nonlinear Dynamics*. 2023; 111(24): 22727-22761.

[62] Mondal B, Thirthar AA, Sk N, Alqudah MA, Abdeljawad T. Complex dynamics in a two species system with Crowley-Martin response function: Role of cooperation, additional food and seasonal perturbations. *Mathematics and Computers in Simulation*. 2024; 221: 415-434.